Molecular Biology of the Cell
Vol. 18, 265–281, January 2007

Regulation of Cdc42 GTPase Activity in the Formation of Hyphae in *Candida albicans*[D]

Helen Court and Peter Sudbery

Department of Molecular Biology and Biotechnology, Sheffield University, Sheffield S10 2TN, United Kingdom

Submitted May 11, 2006; Revised October 20, 2006; Accepted October 26, 2006
Monitoring Editor: Daniel Lew

The human fungal pathogen *Candida albicans* can switch between yeast, pseudohyphal, and hyphal morphologies. To investigate whether the distinctive characteristics of hyphae are due to increased activity of the Cdc42 GTPase, strains lacking negative regulators of Cdc42 were constructed. Unexpectedly, the deletion of the Cdc42 Rho guanine dissociation inhibitor *RDI1* resulted in reduced rather than enhanced polarized growth. However, when cells lacking both Cdc42 GTPase-activating proteins, encoded by *RGA2* and *BEM3*, were grown under pseudohyphal-promoting conditions the bud was highly elongated and lacked a constriction at its base, so that its shape resembled a hyphal germ tube. Moreover, a Spitzenkörper was present at the bud tip, a band of disorganized septin was present at bud base, true septin rings formed within the bud, and nuclei migrated out of the mother cell before the first mitosis. These are all characteristic features of a hyphal germ tube. Intriguingly, we observed hyphal-specific phosphorylation of Rga2, suggesting a possible mechanism for Cdc42 activation during normal hyphal development. In contrast, expression of $Cdc42^{G12V}$, which is constitutively GTP bound because it lacks GTPase activity, resulted in swollen cells with prominent and stable septin bars. These results suggest the development of hyphal-specific characteristics is promoted by Cdc42-GTP in a process that also requires the intrinsic GTPase activity of Cdc42.

INTRODUCTION

Candida albicans is the most common human fungal pathogen, responsible for infections that range from superficial mycoses such as vaginitis to severe, life-threatening bloodstream infections in vulnerable, immunocompromised patients (Beck-Sague and Jarvis, 1993; Kibbler *et al*., 2003). A striking feature of its biology is its capacity to grow in different morphological forms: yeast, pseudohyphae, and hyphae (Berman and Sudbery, 2002; Sudbery *et al*., 2004). The morphology of the yeast form closely resembles that of the budding yeast *Saccharomyces cerevisiae*. Hyphae consist of chains of long cells with unconstricted, parallel-sided walls. Pseudohyphae also consist of chains of elongated cells, but they display constrictions at the mother-daughter cell neck and at septal junctions. In addition to differences in cell shape, hyphae are distinguished from both yeast and pseudohyphae by three further characteristics (Sudbery *et al*., 2004). First, growth is intensely polarized to the hyphal tip and proceeds continuously throughout the cell cycle, whereas the growth of buds in yeast and pseudohyphae is restricted to the tip only for the first part of the cell cycle (Soll *et al*., 1985; Crampin *et al*., 2005). Second, septin rings, which organize the formation of the primary septum, form at the mother-bud neck in yeast and pseudohyphae shortly before bud emergence at the start of the cell cycle (Sudbery, 2001; Warenda and Konopka, 2002). However, hyphal germ tube evagination from an unbudded yeast cell occurs before the start of the cell cycle (Hazan *et al*., 2002). A band of septin bars forms at the base of the germ tube and as it elongates, a true septin ring forms 5–15 μm away from the mother cell (Sudbery, 2001; Warenda and Konopka, 2002). The appearance of this septin ring is coincident with the start of the cell cycle (Finley and Berman, 2005). Third, nuclear division takes place across the mother/bud neck in yeast and pseudohyphae, but within the germ tube in hyphae (Sudbery, 2001). Understanding the molecular mechanisms responsible for these differences will not only increase understanding of this important pathogen, but it may serve as a useful model for fundamental aspects of cell biology relevant to all eukaryotic cells.

We recently showed that polarized growth in *C. albicans* hyphae is driven by a different mechanism compared with that in yeast and pseudohyphae (Crampin *et al*., 2005). Hyphal growth depends on a Spitzenkörper, whereas in yeast and pseudohyphae polarized growth depends on a polarisome. A Spitzenkörper is a vesicle-rich apical body that acts as a vesicle supply center to concentrate the delivery of secretory vesicles to the growing tip (Bartnicki-Garcia *et al*., 1989; Virag and Harris, 2006). First studied in *S. cerevisiae*, the polarisome is a multiprotein complex containing Bni1, Spa2, Bud6, and Pea2 forming a surface crescent at the tip of young buds (Evangelista, 1997; Sheu *et al*., 1998). The polarisome facilitates the nucleation of actin cables by the formin Bni1 (Sagot *et al*., 2002; Evangelista *et al*., 2002). Secretory vesicles are transported along these actin cables by the type V myosin, Myo2, complexed to its regulatory light chain, Mlc1 (Bretscher, 2003).

In *S. cerevisiae*, polarized growth and the formation and organization of the septin rings are ultimately controlled by

This article was published online ahead of print in *MBC in Press* (http://www.molbiolcell.org/cgi/doi/10.1091/mbc.E06–05–0411) on November 8, 2006.

[D] The online version of this article contains supplemental material at *MBC Online* (http://www.molbiolcell.org).

Address correspondence to: Peter Sudbery (p.sudbery@shef.ac.uk).

Abbreviations used: GAP, GTPase-activating protein.

the Cdc42 GTPase (Johnson and Pringle, 1990; Johnson, 1999). Like all Rho-type GTPases, Cdc42 cycles between GDP- and GTP-bound forms. Cdc24 acts as a guanine nucleotide exchange factor (GEF) to mediate the formation of the GTP-bound Cdc42 (Zheng *et al*., 1994; Johnson, 1999). Activation of GTPase activity, to return Cdc42 to the GDP-bound form, is mediated by the GTPase-activating proteins (GAPs) Rga1, Rga2, and Bem3 (Zheng *et al*., 1994; Stevenson *et al*., 1995; Smith *et al*., 2002; Caviston *et al*., 2003). Classically, GTPases such as Cdc42 act as molecular switches, the GTP-bound form being the active state. Thus, Cdc24 would be expected to be a positive regulator and the GAPs to be negative regulators of Cdc42 signaling. As expected, loss of Cdc24 results in a similar phenotype to loss of Cdc42, that is, cells are unable to form buds and mutants arrest as large unbudded cells (Hartwell, 1974; Adams *et al*., 1990).

However, the role of the GAPs is not so straightforward. *S. cerevisiae* mutants lacking Cdc42 GAPs show defects in both bud morphology and septin ring organization (Gladfelter *et al*., 2002; Smith *et al*., 2002; Caviston *et al*., 2003). Septin rings are sometimes absent from the bud neck and found instead at the bud tip or within an elongated daughter cell. In other cells septins remain at the neck but form a misorganized septin band, consisting of longitudinal bars, which resembles the basal septin band that forms in *C. albicans* germ tubes (Sudbery, 2001). Mutations have been isolated in the effector domain of Cdc42, which specifically affect septin ring formation. Two of these mutants, $cdc42^{Y32H}$ and $cdc42^{V36TK94E}$, are defective in GTPase activity and are suppressed by multicopy *RGA1* (Gladfelter *et al*., 2002). Moreover, a temperature-sensitive septin mutant, *cdc12-6*, is suppressed by multicopy *RGA1* or *BEM3* (Caviston *et al*., 2003). These observations suggest that Cdc42-directed GAPs may play a positive role in organizing the septin ring. Two explanations have been advanced for this unexpected conclusion. First, Cdc42 cycling between GTP- and GDP-bound forms may be required for proper septin ring formation (Gladfelter *et al*., 2002). Second, GAPs may directly participate in the formation of septin rings (Caviston *et al*., 2003). These hypotheses are not mutually exclusive.

Further regulation of Cdc42 activity may be imposed by the Rho-guanine dissociation inhibitor (Rho-GDI) Rdi1. Rho-GDIs extract their target Rho-GTPase from membranes and maintain them in the cytosol, block the dissociation of GDP necessary for the exchange of GDP for GTP, and may interfere with association of the GTPase with its targets (DerMardirossian and Bokoch, 2005). Rdi1 is the only *S. cerevisiae* Rho-GDI, and it coimmunoprecipitates with both Cdc42 and Rho1; so, it may regulate both of these GTPases. However, its deletion has no obvious phenotypic effects (Masuda *et al*., 1994; Koch *et al*., 1997).

Cdc42 not only controls septin ring formation and organization but also controls the delivery and docking of secretory vesicles to the bud tip, a process that is required for polarized growth to occur (Pruyne *et al*., 2004). Cdc42 is therefore likely to play a key role in promoting the characteristic aspects of hyphal morphology in *C. albicans*, as hyphal elongation depends on continuous polarized growth toward the hyphal tip (Soll *et al*., 1985; Crampin *et al*., 2005). Several lines of evidence confirm that this is the case. First, in *S. cerevisiae cdc42* alleles have been isolated that specifically reduce pseudohyphal growth, and when strains of *C. albicans* were constructed with the equivalent alleles, the capacity for hyphal growth was greatly reduced (vanden Berg *et al*., 2004). Second, promoter shutdown experiments show that in *C. albicans*, Cdc42 and its GEF Cdc24 are required for viability, and their ectopic expression from a nonnative promoter interferes with hyphal induction (Ushinsky *et al*., 2002; Bassilana *et al*., 2003). Third, expression of $CDC42^{G12V}$, encoding a constitutively GTP-bound form was found to be lethal (Ushinsky *et al*., 2002), as it was in *S. cerevisiae* (Ziman *et al*., 1991). *C. albicans* yeast cells conditionally expressing $Cdc42^{G12V}$ arrested with a multibudded morphology, whereas cells induced to form hyphae were swollen and showed reduced polarity.

These experiments show that proper regulation of Cdc42 is critical for normal hyphal development. In *S. cerevisiae*, loss of all of the Cdc42 GAP proteins encoded by Rga1/2 and Bem3 would be expected to result in elevated levels of activated Cdc42, yet in contrast to the phenotype of cells expressing $CDC42^{G12V}$, cells lacking the Cdc42 GAPs show hyperpolarized bud growth and the ectopic septin ring formation — features reminiscent of hyphal formation in *C. albicans* (Gladfelter *et al*., 2002; Smith *et al*., 2002; Caviston *et al*., 2003). This suggests that the Cdc42 GAPs may play an important role in modulating Cdc42 action with respect to morphological switching. Another protein that may play a role in modulating Cdc42 activity is Rdi1. Here, we investigate the role of Cdc42 GAPs and Rdi1 in *C. albicans* to test the hypothesis that these proteins provide the additional elements of Cdc42 regulation necessary for the control of the morphological transitions between yeast, pseudohyphae, and hyphae.

MATERIALS AND METHODS

Media and Growth Conditions

Unless stated otherwise cultures were grown on YEPD (2% glucose, 2% Difco Bacto peptone, and 1% Difco Bacto yeast extract) plus 80 mg l^{-1} uridine. SD medium consists of 0.67% wt/vol yeast nitrogen base (Difco, Detroit, MI), 2% (wt/vol) glucose, and 80 mg l^{-1} each of histidine, uridine, and arginine. Yeast form growth was promoted by adjusting the pH to 6.0 and incubating at 25°C. Pseudohyphal growth was promoted by adjusting the pH to 6.0 and incubating at 36°C. Hyphal growth was promoted by adjusting the pH to 7.0, adding 20% calf serum and incubating at 37°C.

Techniques for Microscopy

Wide field epifluorescence microscopy was carried out using a Delta Vision Linux IV microscope (Applied Precision Instruments, Seattle, WA) with an Olympus 100× UPlanApo NA 1.35 lens (Olympus, Tokyo, Japan). Images were deconvolved using the SoftWoRx image analysis software supplied with the microscope. Where parts of images were expanded to show greater detail, the SoftWoRx Interpolated Zoom facility was used to smooth pixilation. Unless otherwise stated images are projections of deconvolved Z stacks. Quantification of fluorescence was carried out using the SoftWoRx Data Inspector function by using images that had been deconvolved but not subjected to any other form of processing. Where intensity between images was compared, the images were captured on the same day with the same exposure time. Differential interference contrast (DIC) images were acquired with a DMLB microscope by using a 100× UPlan Apo NA 1.35 objective (Leica, Wetzlar, Germany) and were captured with a model CCD-1800-v camera (Princeton Instruments, Monmouth Junction, NJ) controlled by Openlab version 2.5 software (Improvision, Warwick, United Kingdom). Cell dimensions were measured in cells fixed with 2.5% formaldehyde by using the dimension-measuring facility in Openlab. Where dimensions of strains were directly compared the cultures were grown in parallel on the same day. Images from both the Leica and Delta Vision microscopes were exported as TIFF files, which were edited for size and contrast in Adobe Photoshop version 7.0 (Adobe Systems, Mountain View, CA).

Western Blots

Western blots were carried out as described previously (Wightman *et al*., 2004; Crampin *et al*., 2005). The anti-green fluorescent protein (GFP) monoclonal antibody (mAb) was supplied by Roche Biosciences (Lewes, United Kingdom). Anti tetra-His mAb (QIAGEN, Dorking, Surrey, United Kingdom) was used to recognize Rdi1–6His. Sba1, used as a loading control in Figure 10, is an Hsp90 cochaperone whose total cellular content remains constant under a variety of growth conditions (Millson *et al*., 2005). Anti-Sba1 polyclonal antiserum was a kind gift from P. Piper (Sheffield University, United Kingdom).

Table 1. Strains used in this study

Strain	Genotype	Source or reference
BWP17	*ura3::λimm434/ura3::λimm434 his1::hisG/his1::hisG arg4::hisG/arg4::hisG*	Wilson *et al.* (1999)
CDC10-YFP	BWP17 *CDC10/CDC10-YFP:URA3*	This study
MLC1-YFP	BWP17 *MLC1/MLC1-YFP:URA3*	Crampin *et al.* (2005)
NOP1-YFP	BWP17 *NOP1/NOP1-YFP:URA3*	This study
MET3-YFP-CDC42	BWP17 *CDC42/URA3:MET3-YFP-CDC42*	This study
RGA2-YFP	BWP17 *RGA2/RGA2-YFP:URA3*	This study
BEM3-YFP	BWP17 *BEM3/BEM3-YFP:URA3*	This study
RDI1-YFP	BWP17 *RDI1/RDI1-YFP:URA3*	This study
*rga2*Δ/Δ	BWP17 *rga2::HIS1/rga2::ARG4*	This study
*bem3*Δ/Δ	BWP17 *bem3::HIS1/bem3::ARG4*	This study
*rdi1*Δ/Δ	BWP17 *rdi1::HIS1/rdi1::ARG4*	This study
*swe1*Δ/Δ	BWP17 *swe1::HIS1/swe1::ARG4*	Wightman *et al.* (2004)
*rga2*Δ/Δ *bem3*Δ/Δ	BWP17 *rga2::HIS1/rga2::ARG4 bem3::ura3*(5′Δ)/*bem3::ura3*(5′Δ)	This study
*rga2*Δ/Δ *bem3*Δ/Δ *rdi1*Δ/Δ	BWP17 *rga2::HIS1/rga2::ARG4 bem3::ura3*(5′Δ)/*bem3::ura3*(5′Δ) *rdi1::ura3*(5′Δ)/*rdi1::ura3*(5′Δ)	This study
*rga2*Δ/Δ *bem3*Δ/Δ *swe1*Δ/Δ	BWP17 *rga2::HIS1/rga2::ARG4 bem3::ura3*(5′Δ)/*bem3::ura3*(5′Δ) *swe1::ura3*(5′Δ)/*swe1::ura3*(5′Δ)	This study
*rga2*Δ/Δ *CDC10-YFP*	BWP17 *rga2::HIS1/rga2::ARG4 CDC10/CDC10-YFP:URA3*	This study
*rga2*Δ/Δ *MLC1-YFP*	BWP17 *rga2::HIS1/rga2::ARG4 MLC1/MLC1-YFP:URA3*	This study
*rga2*Δ/Δ *NOP1-YFP*	BWP17 *rga2::HIS1/rga2::ARG4 NOP1/NOP1-YFP:URA3*	This study
*bem3*Δ/Δ *CDC10-YFP*	BWP17 *bem3::HIS1/bem3::ARG4 CDC10/CDC10-YFP:URA3*	This study
*bem3*Δ/Δ *MLC1-YFP*	BWP17 *bem3::HIS1/bem3::ARG4 MLC1/MLC1-YFP:URA3*	This study
*bem3*Δ/Δ *NOP1-YFP*	BWP17 *bem3::HIS1/bem3::ARG4 NOP1/NOP1-YFP:URA3*	This study
*rdi1*Δ/Δ *CDC10-YFP*	BWP17 *rdi1::HIS1/rdi1::ARG4 CDC10/CDC10-YFP:URA3*	This study
*rga2*Δ/Δ *bem3*Δ/Δ *CDC10-YFP*	BWP17 *rga2::HIS1/rga2::ARG4 bem3::ura3*(5′Δ)/*bem3::ura3*(5′Δ) *CDC10/CDC10-YFP:URA3*	This study
*rga2*Δ/Δ *bem3*Δ/Δ *MLC1-YFP*	BWP17 *rga2::HIS1/rga2::ARG4 bem3::ura3*(5′Δ)/*bem3::ura3*(5′Δ) *MLC1/MLC1-YFP:URA3*	This study
*rga2*Δ/Δ *bem3*Δ/Δ *NOP1-YFP*	BWP17 *rga2::HIS1/rga2::ARG4 bem3::ura3*(5′Δ)/*bem3::ura3*(5′Δ) *NOP1/NOP1-YFP:URA3*	This study
*rga2*Δ/Δ *bem3*Δ/Δ *rdi*Δ/Δ *CDC10-YFP*	BWP17 *rga2::HIS1/rga2::ARG4 bem3::ura3*(5′Δ)/*bem3::ura3*(5′Δ) *rdi1::ura3*(5′Δ)/*rdi1::ura3*(5′Δ) *CDC10/CDC10-YFP:URA3*	This study
*rga2*Δ/Δ *bem3*Δ/Δ rdiΔ/Δ*MLC1-YFP*	BWP17 *rga2::HIS1/rga2::ARG4 bem3::ura3*(5′Δ)/*bem3::ura3*(5′Δ) *rdi1::ura3*(5′Δ)/*rdi1::ura3*(5′Δ) *MLC1/MLC1-YFP:URA3*	This study
*rga2*Δ/Δ *bem3*Δ/Δ *swe1*Δ/Δ *CDC10-YFP*	BWP17 *rga2::HIS1/rga2::ARG4 bem3::ura3*(5′Δ)/*bem3::ura3*(5′Δ) *swe1::ura3*(5′Δ)/*swe1::ura3*(5′Δ) *CDC10/CDC10-YFP:URA3*	This study
*rga2*Δ/Δ *bem3*Δ/Δ *swe1*Δ/Δ*MLC1-YFP*	BWP17 *rga2::HIS1/rga2::ARG4 bem3::ura3*(5′Δ)/*bem3::ura3*(5′Δ) *swe1::ura3*(5′Δ)/*swe1::ura3*(5′Δ) *MLC1/MLC1-YFP:URA3*	This study
*rga2*Δ/Δ *bem3*Δ/Δ *MET3-YFP-CDC42*	BWP17 *rga2::HIS1/rga2::ARG4 bem3::ura3*(5′Δ)/*bem3::ura3*(5′Δ) *CDC42/URA3::MET3-YFP-CDC42*	This study
*rdi1*Δ/Δ *RDI1*	BWP17 r*di1::HIS1/rdi1::ARG4/RDI1::URA3*	This study
*rdi1*Δ/Δ *MET3-RDI1*	BWP17 *rdi1::HIS1/rdi1::ARG4/MET3-RDI1::URA3*	This study
*rdi1*Δ/Δ pCIP10	BWP17 *rdi1::HIS1/rdi1::ARG4 rp10::URA3/RP10*	This study
*rdi1*Δ/Δ pCAEXP	BWP17 *rdi1::HIS1/rdi1::ARG4 rp10::URA3/RP10*	This study
*rga2*Δ/Δ *bem3*Δ/Δ *rdi1*Δ/Δ *RDI1*	BWP17 *rga2::HIS1/rga2::ARG4 bem3::ura3*(5′Δ)/*bem3::ura3*(5′Δ) *rdi1::ura3*(5′Δ)/*rdi1::ura3*(5′Δ)/*RDI1::URA3*	This study
*rga2*Δ/Δ *bem3*Δ/Δ *rdi1*Δ/Δ *MET3-RDI1*	BWP17 *rga2::HIS1/rga2::ARG4 bem3::ura3*(5′Δ)/*bem3::ura3*(5′Δ) *rdi1::ura3*(5′Δ)/*rdi1::ura3*(5′Δ)/*MET3-RDI1::URA3*	This study
*rga2*Δ/Δ *bem3*Δ/Δ *rdi1*Δ/Δ pCIP10	BWP17 *rga2::HIS1/rga2::ARG4 bem3::ura3*(5′Δ)/*bem3::ura3*(5′Δ) *rdi1::ura3*(5′Δ)/*rdi1::ura3*(5′Δ) *rp10::URA3/RP10*	This study
*rga2*Δ/Δ *bem3*Δ/Δ *rdi1*Δ/Δ pCAEXP	BWP17 *rga2::HIS1/rga2::ARG4 bem3::ura3*(5′Δ)/*bem3::ura3*(5′Δ) *rdi1::ura3*(5′Δ)/*rdi1::ura3*(5′Δ) *rp10::URA3/RP10*	This study
*rga2*Δ/Δ *bem3*Δ/Δ *MET3-RGA2*	BWP17 *rga2::HIS1/rga2::ARG4/MET3-RGA2::URA3 bem3::ura3*(5′Δ)/*bem3::ura3*(5′Δ)	This study
*rga2*Δ/Δ *bem3*Δ/Δ pCAEXP	BWP17 *rga2::HIS1/rga2::ARG4 bem3::ura3*(5′Δ)/*bem3::ura3*(5′Δ) *rp10::URA3/RP10*	This study
*rga2*Δ/Δ *bem3*Δ/Δ *MET3-BEM3*	BWP17 *rga2::HIS1/rga2::ARG4 bem3::ura3*(5′Δ)/*bem3::ura3*(5′Δ)/*MET3-BEM3::URA3*	This study
CaSU64	*ura3/ura3 CDC42/cdc42::hisG PCK1-CaCDC42^{G12V}::hisG-URA3-hisG*	Ushinsky *et al.* (2002)
CaSU64:*MLC1-YFP*	*ura3/ura3 CDC42/cdc42::hisG PCK1-CaCDC42^{G12V}::hisG MLC1/MLC1-YFP:URA3*	This study
CaSU64:*CDC10-YFP*	*ura3/ura3 CDC42/cdc42::hisG PCK1-CaCDC42^{G12V}::hisG CDC10/CDC10-YFP:URA3*	This study
*rga2*Δ/*RGA2*	BWP17 *rga2::HIS1/RGA2*	This study
*bem3*Δ/*BEM3*	BWP17 *bem3::HIS1/BEM3*	This study
*bem3*Δ/Δ *rga2*Δ/*RGA2*	BWP17 *bem3::HIS1/bem3::ARG4 rga2::ura3*(5′Δ)/*RGA2*	This study
*rga2*Δ/*rga2*Δ *bem3*Δ/*BEM3*	BWP17*rga2::HIS1/rga2::ARG4 bem3::ura3*(5′Δ)/*BEM3*	This study
*rga2*Δ/*rga2^{K1061A}*	BWP17 *rga2::HIS1/rga2^{K1061A}::ARG4*	This study

Continued

Table 1. *Continued*

Strain	Genotype	Source or reference
rga2Δ/rga2^{R1015L}	BWP17 *rga2::HIS1/rga2^{R1015L}::ARG4*	This study
bem3Δ/Δ rga2Δ/rga2^{K1061A}	BWP17 *bem3::HIS1/bem3::ARG4 rga2::ura3*(5'Δ)*/ rga2^{K1061A}::URA3*	This study
bem3Δ/Δ rga2Δ/rga2^{R1015L}	BWP17 *bem3::HIS1/bem3::ARG4 rga2::ura3*(5'Δ)*/ rga2^{R1015L}::URA3*	This study
bem3Δ/bem3^{K1025A}	BWP17 *bem3::HIS1/bem3^{K1025A}::ARG4*	This study
bem3Δ/bem3^{R985L}	BWP17 *bem3::HIS1/bem3^{R985L}::ARG4*	This study
rga2Δ/rga2Δ bem3Δ/bem3^{K1025A}	BWP17 *rga2::HIS1/rga2::ARG4 bem3::ura3*(5'Δ)*/bem3^{K1025A}::URA3*	This study
rga2Δ/rga2Δ bem3Δ/bem3^{R985L}	BWP17 *rga2::HIS1/rga2::ARG4 bem3::ura3*(5'Δ)*/bem3^{R985L}::URA3*	This study
MET3-YFP-CDC42 RDI1-6HIS	BWP17 *CDC42/URA3:MET3-YFP-CDC42 RDI1/RDI1-6HIS::ARG4*	This study

Strain Construction

Strains constructed are listed in Table 1, and the oligonucleotides used are listed in the Supplemental Table 1. Single mutant strains were constructed by sequential deletion of both alleles in the parental strain BWP17 (Wilson *et al.*, 1999). Double and triple mutant strains were constructed using the recyclable *URA3* cassette *URA3-dpl200* (Wilson *et al.*, 2000). Transformants were screened for transplacement of the targeted gene by using a 5′ primer that annealed within the selectable marker of the transplacing cassette and a 3′ primer that annealed downstream of the deleted gene. Positive clones were further screened using polymerase chain reaction (PCR) primers that annealed upstream and downstream of the deleted gene. A unique restriction site was used to distinguish the disruption cassette from the wild-type gene if they were predicted to be of the same size. When the *URA3* marker was recycled using 5-fluoroorotic acid (FOA), correct excision of the *URA3* gene was confirmed by PCR by using a 5′ primer that annealed within the portion of the *URA3* gene that remained after the recombination event selected by FOA, and a 3′ primer that annealed downstream of the targeted gene. Finally, the complete absence of a gene was confirmed using PCR primers that annealed within the deleted region. The absence of a PCR product, when it was present in an appropriate positive control, confirmed the gene had been deleted. The phenotypes reported here were observed in two independent transformants in each case. To confirm that phenotypes were due to the loss of gene function and not to accidental changes that occurred during genetic manipulation, wild-type copies of the genes were reintroduced into the deleted strains. This was done in two ways. In *RDI1*, the promoter and open reading frame (ORF) were amplified by PCR into CIP10 and reintegrated at the RP10 locus (Brand *et al.*, 2004). Second, in *RGA2*, *BEM3*, and *RDI1*, the coding region was placed under the control of the *MET3* promoter by cloning the ORF, amplified by PCR, into pCaEXP, which was then targeted to the RP10 locus (Care *et al.*, 1999). C-terminal fusions to yellow fluorescent protein (YFP) and cyan fluorescent protein (CFP), and N-terminal *MET3* promoter-YFP fusions were constructed using linear cassettes generated by PCR as described previously (Gerami-Nejad *et al.*, 2001, 2004).

Site-directed Mutagenesis

For site-directed mutagenesis the C-terminal section containing the target site was amplified by PCR and cloned into a pCR2.1-TOPO vector (Invitrogen, Paisley, United Kingdom). Site-directed mutagenesis was carried out a QuikChange II site-directed mutagenesis kit (Stratagene, La Jolla, CA) according to the manufacturer's instructions. Oligonucleotide primers are listed in Supplemental Table 1. The whole mutated sequence was resequenced to verify the desired point mutation and to ensure that no other changes had been introduced inadvertently. The mutated sequence was then subcloned into a pFA *ARG*4 or pFA *URA*3 plasmid (Gola *et al.*, 2003). Transplacements were carried out by PCR by using a forward primer that annealed upstream of the point mutation and a reverse primer that annealed downstream of the selectable marker in the pFA plasmid, and which also contained a 5′ extension derived from the sequence downstream of the stop codon of the target gene. Transplacements were screened by appropriate PCR assays as described above. The mutated sequence in putative mutants was reamplified by PCR and resequenced to confirm the mutation had been introduced and that the reading frame had been maintained.

RESULTS

Morphology of C. albicans Mutants Lacking the Cdc42 GAPs

Regulation of Cdc42 activity and expression is clearly important for normal hyphal morphogenesis (see Introduction). An increase in Cdc42-GTP levels would be predicted to result in an enhancement of polarized growth and to change the pattern of septin ring formation, possibly resulting in the acquisition of hyphal characteristics in conditions when hyphae would not normally form. Indeed, the phenotype of *S. cerevisiae* cells lacking Cdc42 GAPs is reminiscent of some aspects of *C. albicans* hyphae. We therefore sought to investigate the effect of removing these negative regulators of Cdc42 on the morphology and pattern of septin localization in *C. albicans* cells growing in yeast, hyphal, and pseudohyphal conditions. Additionally, we were interested in investigating the role of the *C. albicans* Rdi1 homologue because it may provide an additional element of negative Cdc42 regulation.

The annotation of the *C. albicans* genome sequence identified single homologues of the *S. cerevisiae BEM3*, *RDI1*, and the *RGA1/2* gene pair (Braun *et al.*, 2005). We verified these gene notations by carrying out a BLASTP search using the predicted *S. cerevisiae* protein sequence to search the *C. albicans* genome for predicted proteins showing similar sequences. *Ca*Rga2 (orf19.4593) is 23% identical and 39% similar to *Sc*Rga2 over 1138 residues (p = 3E-33). Because the *C. albicans* orf19.4593 shows a slightly greater similarity to *S. cerevisiae RGA2* compared with *Sc*Rga1, the *C. albicans* gene is named *RGA2*. *Ca*Bem3 is 24% identical and 43% similar over 1088 residues to *ScBem3* (p = 5E-55). No other *C. albicans* proteins with GAP domains showed significant homologies to ScRga2 or ScBem3 (E values < -10). To investigate the role of these proteins during morphogenesis, we constructed mutants in which the encoding genes were deleted both singly and in combination. We also constructed strains in which these mutations were combined with deletions of *SWE1* to investigate whether the mutant phenotypes were due to the operation of the Swe1-dependent morphogenesis checkpoint (Lew and Reed, 1995). To monitor the effect of the mutations on septin ring, Spitzenkörper formation, and nuclear division we introduced *CDC10-YFP*, *MLC1-YFP*, and *NOP1-YFP* alleles, respectively, into these strains. A full list of the genotypes of the strains constructed is shown in Table 1.

During yeast phase growth, loss of Bem3 had little effect on cell morphology compared with the parent BWP17 strain, and septin rings formed normally (Figure 1, A and B). Loss of Rga2 resulted in a uniform population of elongated yeast cells although septin rings still formed between mother and daughter cells and the bud necks looked normal (Figure 1C). Loss of both Rga2 and Bem3 resulted in a small number of cells having highly polarized buds that lack constrictions at the junction with the mother cell (Figure 1D). In these cells, an ectopic septin ring formed in the elongated bud. In some cells, the bud swelled immediately distal to this ring (Figure 1D, arrow). Loss of Swe1 did not reverse the phenotype resulting from loss of the GAPs, showing that the elongated

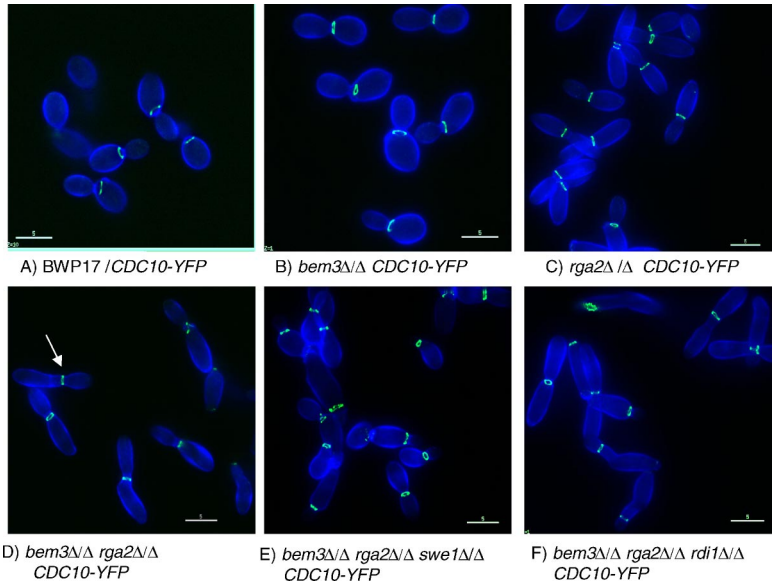

Figure 1. Phenotype of yeast cells lacking the Cdc42 GAPs Rga2 and Bem3. Mutants lacking Rga2 form elongated cells (C) in a Swe1-independent manner (E). Elongation is not enhanced by deletion of *RDI1* (F). Septin rings form at the bud neck (green), except for some *bem3*Δ/Δ *rga2*Δ/Δ mutants cells that show ectopic septin rings located distal to an elongated bud lacking a constriction at its neck and proximal to a bud showing isotropic growth (arrowed in D). Yeast cells of the indicated genotype were grown for 2.5 h after inoculation of an overnight culture into YEPD at 25°C to promote yeast growth. Cells were counterstained with calcofluor white (blue) and examined with a Delta Vision microscope. Bars, 5 μm.

cell phenotype is not a result of the Swe1-dependent morphogenesis checkpoint (Figure 1E). Thus, Rga2 apparently plays a direct role in controlling bud shape. Finally, loss of Rdi1 did not further exacerbate the elongation resulting from loss of the Cdc42 GAPs (Figure 1F). Cells were still elongated and septin rings formed ectopically in some cells.

The morphology of *C. albicans* is sensitive to small changes in environmental pH and temperature and to the nutritional richness of the culture medium. On rich YEPD medium at pH 4.0, 30°C, cells grow predominantly in the yeast form. As temperature and pH are increased, there is a progressive change to pseudohyphal forms. On YEPD at pH 5.0, 36°C, cells grow as short pseudohyphae. On YEPD at pH 6.0, 36°C, cells grow as long pseudohyphae with 10–20% cells growing as hyphae (Sudbery, 2001). Hyphae are induced by growth on YEPD at pH 7.0, 37°C, plus 20% serum. To investigate whether cells lacking Cdc42 GAPs acquire hyphal characteristics under conditions when hyphae do not normally form, we investigated the morphology of mutants in pseudohyphal-promoting conditions. Parental, the *bem3*Δ/Δ *rga2*Δ/Δ double mutant strain, and *bem3*Δ/Δ and the *rga2*Δ/Δ single mutant strains were grown to saturation in YEPD medium under conditions that promote yeast form growth, and the yeast cells were then reinoculated into YEPD medium and cultured in conditions favoring pseudohyphal growth. We report here in detail on experiments where cells were grown on YEPD at pH 6.0, 36°C. However, we obtained similar results with cultures grown on YEPD at pH 5.0, 36°C. In such experiments, pseudohyphal cells evaginate buds 40–50 min after reinoculation into fresh medium (Sudbery, 2001). After evagination, samples were withdrawn at intervals and analyzed to record the dimensions of the hyphal germ tube or pseudohyphal bud. Loss of Cdc42 GAPs had a major effect on the morphology of cells grown in conditions that normally induce pseudohyphal growth (Figure 2). Two differences are apparent in the shape of parental BWP17 cells in Figure 2A, and the mutants lacking Cdc42 GAPs shown in Figure 2, C–E. First, the BWP17 cells show constrictions at the mother bud neck (Figure 2A), which are absent in cells lacking both of the Cdc42 GAPs (Figure 2E) but not in cells lacking only one or other of the GAPs (Figure 2, C and D). Second, cells of the double *bem3*Δ/Δ *rga2*Δ/Δ mutant, and to a lesser extent the *rga2*Δ/Δ single mutant, are longer and thinner than the BWP17 cells. Both of these differences are characteristics that distinguish hyphae (Figure 2B) from pseudohyphae (Figure 2A).

Table 2 shows the results of quantification carried out to record the differences in cell length, width, and the ratio of length to width of the first pseudohyphal bud of the above-mentioned strains. The length-to-width ratio serves as a convenient parameter to record the increased length and decreased width of hyphal germ tubes compared with pseudohyphal buds. Measurements in Table 2 were made 100 min after inoculation. Similar measurements recorded at other time points throughout the time course showed a similar trend (data not shown). The quantification showed that the first pseudohyphal bud of the *rga2*Δ/Δ mutant, but not the *bem3*Δ/Δ mutant, had a greater length and lesser width than the parental BWP17 cells (length-to-width ratios: BWP17 = 2.9 ± 0.4, *rga2*Δ/Δ = 3.9 ± 0.4, and *bem3*Δ/Δ = 3.0 ± 0.4). The double mutant lacking all Cdc42 GAP activity (*bem3*Δ/Δ *rga2*Δ/Δ) showed a further increase in the length-to-width ratio compared with the *rga2*Δ/Δ and *bem3*Δ/Δ single mutants (4.6 ± 0.4) after 100 min. Together, these data show that loss of Cdc42 GAP activity results in a change in the morphology of pseudohyphae so that they acquire characteristics of true hyphae, being longer and thinner than wild-type pseudohyphae and lacking a constriction at the mother-bud neck. However, the phenotype of the *bem3*Δ/Δ *rga2*Δ/Δ double mutant growing in pseudohyphal conditions was still different from that when it was growing in hyphal conditions (Figure 2, E and F). Indeed, the phenotype of *bem3*Δ/Δ *rga2*Δ/Δ mutant growing in hyphal-inducing conditions was indistinguishable from the BWP17 parental strain (length-to-width ratios: BWP17 = 10.4 ± 0.6 and *bem3*Δ/Δ *rga2*Δ/Δ = 10.4 ± 0.9). So, the Cdc42 GAPs are not required for hyphal formation in hyphal-inducing conditions, but in their absence, a more hyphal-like shape develops in pseudohyphal conditions, suggesting that Cdc42 GAPs have a role in regulating the processes that lead to the characteristic hyphal morphology.

As a putative Cdc42 guanine dissociation inhibitor, Rdi1 might be expected to act as a negative regulator of Cdc42, so that its loss would further exacerbate the phenotype of the double mutant lacking GAP activity. Because Rdi1 has been shown to interact with both Rho1 and Cdc42 in *S. cerevisiae*,

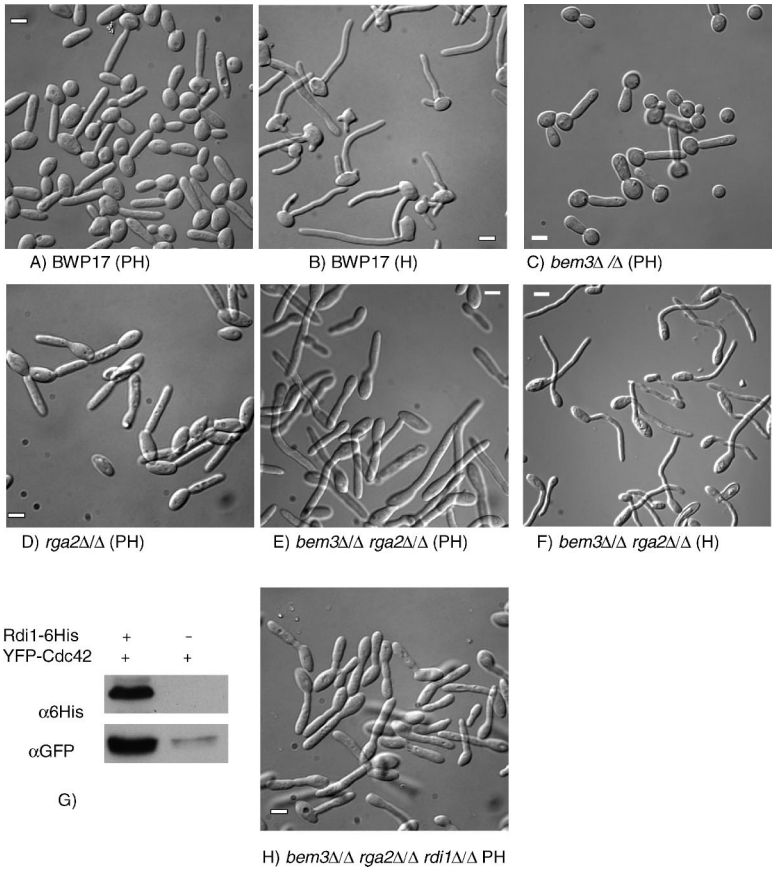

Figure 2. Phenotype of mutants lacking Cdc42 GAPs and Rdi1 in conditions promoting pseudohyphal growth. Appearance of BWP17 cells growing in pseudohyphal-inducing conditions (A) or hyphal-inducing conditions (B). When grown in pseudohyphal-inducing conditions the buds of *rga2*Δ/Δ and *bem3*Δ/Δ *rga2*Δ/Δ cells (D and E) were more elongated and narrower than those of parental cells (A). Note that constrictions are present at the bud neck in the single mutants (C and D) that are absent in the double mutant (E). When *bem3*Δ/Δ *rga2*Δ/Δ cells were grown in hyphal-inducing conditions they formed normal germ tubes (F). YFP-Cdc42 copurifies with Rdi-6His showing that Rdi1 physically associates with Cdc42 (G). The buds of a *bem3*Δ/Δ *rga2*Δ/Δ *rdi1*Δ/Δ mutant were less elongated than a *bem3*Δ/Δ *rga2*Δ/Δ mutant (compare E with H). All images were obtained by DIC microscopy by using samples fixed 100 min after reinoculation. PH, pseudohyphal-inducing conditions (YEPD, pH 6.0, 36°C). H, hyphal-inducing conditions (YEPD, pH 7.0, plus 20% serum, 37°C). (G) Soluble protein extracts of yeast cells expressing YFP-Cdc42 with, or without, a Rdi1–6His fusion were fractionated on a His-select column (Sigma-Aldrich, St. Louis, MO) and the eluate challenged with a mixture of two anti-GFP monoclonal antibodies (αGFP) (Roche Biosciences) or an anti-tetra His mAb (QIAGEN). Scale bars = 5 μm.

we determined whether Rdi1 interacts with Cdc42 in *C. albicans*. Figure 2G shows that YFP-Cdc42 physically associates with Rdi1–6His in *C. albicans* yeast cells, confirming that Rdi1 does interact with Cdc42. We examined the phenotype of a *bem3*Δ/Δ *rga2*Δ/Δ *rdi1*Δ/Δ triple mutant and were surprised to observe that under pseudohyphal conditions, the mutant had a less extreme phenotype than the *bem3*Δ/Δ *rga2*Δ/Δ double mutant (Figure 4H and Table 3). Thus, Rdi1 does not simply act as a negative regulator of Cdc42.

The extensive genetic manipulation required to generate strains lacking both Rga2 and Bem3 may have introduced changes other than those which were intended. To verify that the phenotypes we observed were solely caused by the absence of both of these Cdc42 GAPs, we separately reintroduced *RGA2* and *BEM3* into the *bem3*Δ/Δ *rga2*Δ/Δ strain under the control of the regulatable *MET3* promoter (Care *et al*., 1999). As expected, expression of either *RGA2* or *BEM3* in the *bem3*Δ/Δ *rga2*Δ/Δ mutant growing under pseudohyphal-promoting conditions resulted in a reduction in the degree of polarized growth and restored constrictions at the mother/bud neck (Supplemental Figure 1). Thus the characteristic phenotype of the *bem3*Δ/Δ *rga2*Δ/Δ mutant is solely due to the absence of both Rga2 and Bem3. In a similar way we showed that the effects of the *rdi1*Δ/Δ allele on the phenotype of a *bem3*Δ/Δ *rga2*Δ/Δ mutant was due solely due to loss of Rdi1 (data not shown).

The experiments reported in Figure 2 focus on the role of the Cdc42 GAPs during the establishment of hyphal or pseudohyphal growth during the first few cell cycles after outgrowth from unbudded yeast cells. To investigate the effect over a longer time frame, we investigated the response of the mutants to growth on solid Spider medium, which promotes filamentous growth from colony edges (Liu *et al*., 1994). (We refer to "filamentous growth" here because the nature of the colony outgrowths on Spider medium has not so far been characterized as hyphae or pseudohyphae.) The *bem3*Δ/Δ *rga2*Δ/Δ double mutant, and to a lesser extent, the *bem3*Δ/Δ and *rga2*Δ/Δ single mutants, showed enhanced filamentation compared with the parental strain (Figure 3, A–D). Thus, loss of Cdc42 GAPs not only enhances polarized growth in the short-term but also results in sustained enhancement of filamentous growth on Spider medium. Consistent with its effect on polarized growth in the yeast and pseudohyphal forms, loss of Rdi1 greatly reduced filamentous growth; indeed, the triple mutant lacking both the Cdc42 GAPs and Rdi1 showed less filamentation than the parental BWP17 strain (Figure 3, E and F). Loss of Swe1 abolished filament formation even in the double mutant lacking the Cdc42 GAPs; Figure 3, G and H). This result is surprising because we had previously found that *swe1*Δ/Δ mutants formed germ tubes normally in liquid culture when challenged with serum (Wightman *et al*., 2004), although others have found that the rate of hyphal elongation, and the degree of filamentation on serum agar is reduced in a strain lacking Swe1 (Umeyama *et al*., 2005). Note that the *swe1*Δ/Δ mutation in the strain shown in Figure 3G was generated independently of the *swe1*Δ/Δ mutation in the strain shown in Figure 3H.

In the Absence of the Cdc42 GAPs, Spitzenkörpers Form Ectopically

The hyphal-like morphology displayed by mutants lacking the Cdc42 GAPs growing in pseudohyphal conditions may be due to the formation of a Spitzenkörper. To see whether

Table 2. Dimensions of cells lacking Cdc42 GAPs growing in pseudohyphal conditions

Strain	Length (μm)	Width (μm)	Length/ width	% Septa not at bud neck
BWP17	9.5 ± 1.0	3.4 ± 0.1	2.9 ± 0.4	N.D.
BWP17 (H)	17.5 ± 1.1	1.7 ± 0.04	10.4 ± 0.6	N.D.
*bem3*Δ/Δ	9.4 ± 0.9	3.2 ± 0.1	3.0 ± 0.4	N.D.
*rga2*Δ/Δ	10.7 ± 1.0	2.8 ± 0.1	3.9 ± 0.4	N.D.
*.rga2*Δ/*rga2*^{K1061A}	10.8 ± 1.0	2.7 ± 0.1	4.0 ± 0.4	N.D.
*rga2*Δ/*rga2*^{R1015L}	10.8 ± 0.7	2.9 ± 0.1	3.8 ± 0.3	N.D.
*rga2*Δ/Δ *bem3*Δ/Δ	13.4 ± 0.8	2.9 ± 0.1	4.6 ± 0.4	63
*rga2*Δ/Δ *bem3*/Δ (H)	17.6 ± 1.1	1.7 ± 0.04	10.4 ± 0.9	N.D.
*rga2*Δ/Δ *bem3*Δ/ *BEM3*	10.7 ± 0.9	3.1 ± 0.1	3.5 ± 0.3	21
*bem3*Δ/Δ *rga2*Δ/ *RGA2*	8.8 ± 1.0	3.3 ± 0.1	2.7 ± 0.3	2
*rga2*Δ/Δ *bem3*Δ/ *bem3*^{K1025A}	12.8 ± 0.7	3 ± 0.1	4.4 ± 0.3	69
*rga2*Δ/Δ *bem3*Δ/ *bem3*^{R985L}	12.2 ± 0.7	3 ± 0.1	4.1 ± 0.4	64
*bem3*Δ/Δ *rga2*Δ/ *rga2*^{K1061A}	12.9 ± 0.8	2.9 ± 0.1	4.5 ± 0.3	79
*bem3*Δ/Δ *rga2*Δ/ *rga2*^{R1015L}	13.8 ± 0.9	2.8 ± 0.1	5.0 ± 0.4	67

N.D., not done.

Measurements were made on 50 cells 100 min after inoculation of stationary phase cells into cells growing in pseudohyphal conditions (YEPD, pH 6.0, 36°C) or, where indicated (H), into hyphal inducing conditions (YEPD, pH 7.0, plus 20% serum). Errors are 95% confidence limits. Quantitation of percentage of septin rings not at the bud neck for BWP17, *bem3*Δ/Δ, *rga2*Δ/Δ, and *bem3*Δ/Δ *rga2*Δ/Δ are shown in Figure 6D.

this is the case, we examined the mutants lacking the Cdc42 GAPs to see whether a Spitzenkörper formed during conditions of pseudohyphal growth. In *C. albicans*, the Spitzenkörper can be visualized by the localization of Mlc1-YFP to a discrete spot just behind the hyphal tip (Figure 4J) (Crampin *et al*., 2005), whereas in pseudohyphae Mlc1-YFP localizes to an apical crescent characteristic of a polarisome (Figure 4, A and B) (Crampin *et al*., 2005). Figure 4, C and D, shows that in most *bem3*Δ/Δ *rga2*Δ/Δ *MLC1/MLC1-YFP* cells growing in pseudohyphal-promoting conditions, Mlc1-YFP localizes to a discrete apical spot characteristic of a Spitzenkörper. Another way to visualize the Spitzenkörper is by staining with the amphiphilic membrane dye FM4-64 (Fischer-Parton *et al*., 2000; Crampin *et al*., 2005). Figure 4E shows that FM4-64 colocalizes with Mlc1-YFP to a discrete spot in the *bem3*Δ/Δ *rga2*Δ/Δ *MLC1/MLC1-YFP* mutant growing in pseudohyphal-promoting conditions. Thus the loss of the Cdc42 GAPs Rga2 and Bem3 results in the formation of a Spitzenkörper in conditions where it would not normally be present. Mlc1-YFP also localized to a Spitzenkörper-like structure in many cells lacking only one or other of the Cdc42 GAPs (Figure 4, F and G).

Apart from morphology and Mlc1-YFP localization, the Spitzenkörper and polarisome are distinguished by two further characteristics. First, the Spitzenkörper is present continuously so that at the end of the cell cycle Mlc1-YFP is present simultaneously in the Spitzenkörper and in the contractile cytokinetic ring. However during pseudohyphal growth, Mlc-YFP localization to the polarisome disappears before fluorescence is observed at the cytokinetic ring (Crampin *et al*., 2005). Second, the maximum fluorescence intensity of Mlc1-YFP in the Spitzenkörper is approximately threefold greater compared with that in the polarisome (Crampin *et al*., 2005). In the *bem3*Δ/Δ *rga2*Δ/Δ mutant growing under pseudohyphal-inducing conditions, Mlc1-YFP localization to the Spitzenkörper was indeed found to persist as Mlc1-YFP appeared in the cytokinetic ring (Figure 4I). We quantified the morphology and maximum fluorescence intensity of Mlc1-YFP at the tips of pseudohyphal cells of parental and mutant strains at intervals after inoculation of unbudded yeast cells into pseudohyphal growth conditions. For comparison, we also analyzed a parallel culture of BWP17 cells growing as hyphae. Each tip was classified according to whether it displayed a spot, crescent, or showed no fluorescence. We verified these assignments by showing that there was a consistent correlation between the fluorescence intensity and the pattern of localization assigned (see legend to Figure 5). The pattern of Mlc1-YFP localization in parental BWP17 cells growing as hyphae and pseudohyphae is shown in Figure 4, A and B, respectively. As we reported previously (Crampin *et al*., 2005), in cells growing in the hyphal form, Mlc1-YFP localized to an apical spot that persisted over the whole of the first cell cycle in >80% of the cells (Figure 5A). The remaining 20%, which displayed a crescent that disappeared at 80 min, was probably due to the small proportion of pseudohyphae that are present in such cultures (Sudbery, 2001). In contrast, in the pseudohyphal culture most cells displayed a crescent at early time points, which disappeared at the end of the first cycle (100 min), before reappearing as the second cycle commenced (110–130 min).

Figure 5C shows that in the *bem3*Δ/Δ *rga2*Δ/Δ mutant, the proportion of cells displaying a spot morphology dipped at the end of the first cell cycle (100 min), but instead of apical Mlc1-YFP disappearing completely, the proportion of cells displaying a crescent showed a compensatory increase. Thus, some cell cycle regulation remains in cells lacking Cdc42 GAPs, but unlike pseudohyphae, apical Mlc1-YFP localization persists throughout the cell cycle. Consistent with the Spitzenkörper-like organization of Mlc1-YFP in *bem3*Δ/Δ *rga2*Δ/Δ mutants, the intensity of fluorescence at the tip was also found to be similar to that of wild-type hyphae and consistently over three- to fourfold greater than that of BWP17 pseudohyphal cells (Figure 5D). Figure 5B shows that a proportion of small pseudohyphal buds displayed an Mlc1-YFP spot rather than a crescent. However, as we observed previously (Crampin *et al*., 2005), the mean of the peak fluorescence intensity of these spots (194 ± 41) was much less than that of the spots in the BWP17 hyphae (538 ±

Table 3. Effect of an *rdi1*Δ/Δ mutation on cell morphology

Strain	Length	Width	Length/ width
BWP17 pseudohyphal form	7.8 ± 0.9	2.6 ± 0.1	3.0 ± 0.4
*rdi1*Δ/Δ	7.9 ± 0.8	2.8 ± 0.1	2.9 ± 0.3
*rga2*Δ/Δ *bem3*Δ/Δ	11.3 ± 1.0	2.1 ± 0.1	5.4 ± 0.4
*rga2*Δ/Δ *bem3*Δ/Δ *rdi1*Δ/Δ	9.2 ± 0.7	2.4 ± 0.1	3.9 ± 0.3
BWP17 (H)	17.0 ± 1.5	1.7 ± 0.06	10.3 ± 0.9

Measurements were made on 50 cells 100 min after inoculation of stationary phase cells into pseudohyphal-inducing conditions (YEPD, pH 6.0, 36°C), or, where indicated (H), into hyphal inducing conditions (YEPD, pH 7.0, plus 20% serum). Errors are 95% confidence limits.

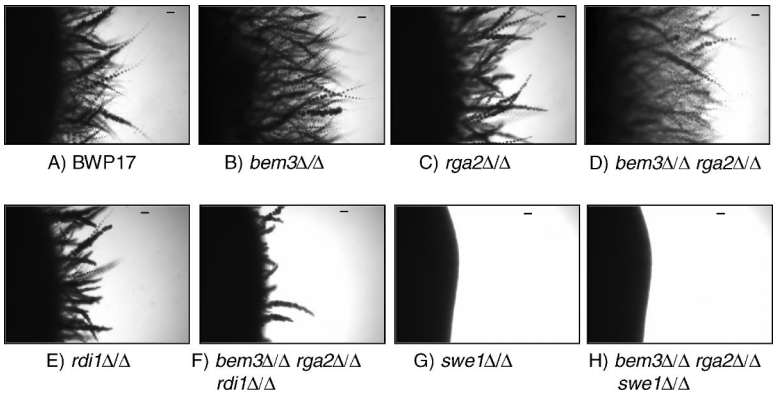

Figure 3. Cells lacking Cdc42 GAPs show greater filamentation on solid Spider medium. Cells of the indicated genotype were cultured on Spider medium (Liu *et al*., 1994) for 5 d and imaged using a Leica DMLB microscope with a 2.5× lens. Bars, 20 μm.

39) or the spots in *bem3*Δ/Δ *rga2*Δ/Δ mutant growing in pseudohyphal-inducing conditions (656 ± 52).

We also quantified the localization of Mlc1-YFP in *bem3*Δ/Δ and *rga2*Δ/Δ single mutants (Figure 5, E–F). In both cases, a spot was observed in about half of the cells immediately after evagination, but the frequency decreased at later times and the proportion of cells displaying a crescent was consistently higher than the double mutant lacking both Cdc42 GAPs. However, unlike the parental strain, some form of apical localization persisted throughout the cell cycle in most cells. Finally, we quantified the localization of Mlc1-YFP in the *bem3*Δ/Δ *rga2*Δ/Δ *rdi1*Δ/Δ triple mutant (Figure 5G). This showed a similar distribution to the *bem3*Δ/Δ *rga2*Δ/Δ double mutant. Thus, loss of Rdi1 does not affect the proportion of cells displaying a Spitzenkörper, so the degree of polarized growth must be reduced for some other reason.

The Pattern of Septin Localization Is Altered in the Absence of Cdc42 GAPs

In addition to the shape, a second defining characteristic of hyphal germ tubes is that the septin ring forms within the germ tube where it organizes the formation of the primary septum during cytokinesis. Moreover, a septin band, consisting of longitudinal bars, forms at the base of the germ tube just after evagination, which disappears as the septin ring forms. In contrast, the septin ring forms at the mother bud neck in pseudohyphae (Sudbery, 2001). To investigate whether Rga2 and Bem3 also regulate this aspect of hyphal growth, and have a role in positioning the site of septin ring formation, we examined the pattern of septin ring localization in wild-type and mutant *C. albicans* cells expressing Cdc10-YFP during growth in pseudohyphal-promoting growth conditions (Figure 6, A–E). As expected, the septin ring formed at the mother-bud neck in all parental BWP17 cells (Figure 6, A and D). However, in cells lacking both Cdc42 GAPs the septin ring formed within the elongated pseudohyphal bud and away from the neck in virtually all cells (Figure 6, B and D). Furthermore, just after evagination of germ tubes, septin bars formed at the base of the bud and a septin cap was transiently visible at the bud tips (Figure 6E). Interestingly, in the *bem3*Δ/Δ and *rga2*Δ/Δ single mutants the septin ring formed at the mother-bud neck in most cells (Figure 6D). Thus, the Cdc42 GAPs are required for the normal regulation of septin ring localization, but the two Cdc42 GAPs are apparently redundant with respect to this function. The pattern of septin localization in the double mutant lacking both Cdc42 GAPs was not affected by the additional loss of Rdi1 (Figure 6D). Consistent with the ectopic position of septin rings, we also observed that Mlc1-YFP in the contractile cytokinetic ring was located within the germ tube instead of the bud neck location expected in pseudohyphae (Figure 4I).

In *S. cerevisiae*, the *cdc42*^{V36T,K94E} mutation causes septin rings to form ectopically in an elongated bud in a Swe1-dependent manner (Gladfelter *et al*., 2005). However, it has also been reported that the ectopic septin rings that form in *S. cerevisiae* cells lacking all Cdc42 GAPs is not Swe1 dependent (Caviston *et al*., 2003). In agreement with the latter observation, we found that the localization of the septin ring within the pseudohyphal bud of *C. albicans* cells lacking Cdc42 GAPs was not Swe1 dependent (Figure 6, C and D).

Nuclear Division Occurs within the Germ Tube of Mutants Lacking Cdc42 GAPs

In pseudohyphae mitosis takes place across the mother-bud neck, but in hyphae nuclei migrate out of the mother cell and mitosis takes place within the germ tube, after which one nucleus returns to the mother cell. Thus, the pattern of nuclear division provides another characteristic that distinguishes hyphae from pseudohyphae. We investigated the pattern of mitosis in *bem3*Δ/Δ *rga2*Δ/Δ cells and parental BWP17 cells, growing in pseudohyphal conditions by expressing Nop1-YFP, a nucleolar protein that can be used to visualize nuclei in living cells (Crampin *et al*., 2005). Unbudded cells from an overnight culture were reinoculated into conditions promoting pseudohyphal growth and the position of the nuclei determined between 100 and 120 min after inoculation, the period during which the majority of cells underwent the first mitosis. Cells that contained either a single nucleus that was located within the germ tube, or contained two nuclei, both of which were in the germ tube, could be confidently scored as cells where mitosis took place in the germ tube. In cells where the nucleus was positioned across the mother bud neck, the site of mitosis cannot be ascertained with certainty, because these cells could either be cells where mitosis is taking place at this position, or they could be cells where the nucleus would continue to migrate into the germ tube. As expected, the nucleus was positioned across the mother bud neck in parental BWP17 cells, consistent with mitosis occurring at this position (Sudbery, 2001) (Figure 7A). In contrast, mitosis took place within the germ tube in the *bem3*Δ/Δ *rga2*Δ/Δ mutant cells growing in pseudohyphal conditions (Figure 7B). Quantification at three separate time points showed that ~20% of *bem3*Δ/Δ *rga2*Δ/Δ cells were undergoing mitosis within the germ tube compared with <1% of parental BWP17 cells (Figure 7C). In contrast, more nuclei were positioned across the mother bud

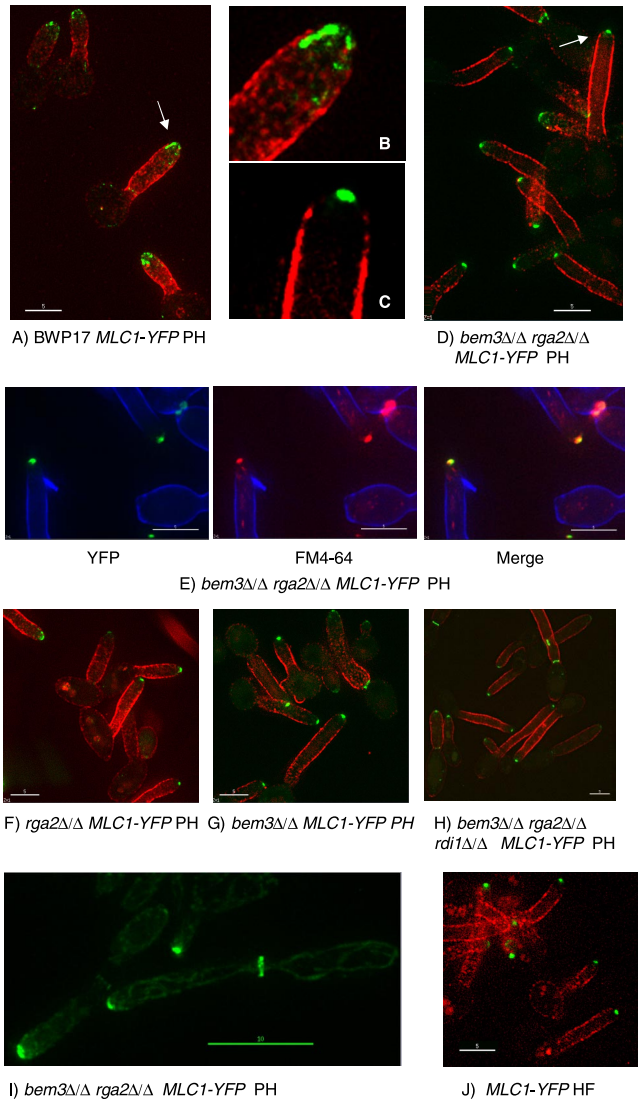

Figure 4. Cells lacking the Cdc42 GAPs Rga2 and Bem3 form a Spitzenkörper in pseudohyphal growth conditions. In BWP17 hyphae, Mlc1-YFP localizes to a spot at, or just behind, the hyphal tip (J), whereas in BWP17 pseudohyphae, Mlc1-YFP localizes to a surface crescent or shows no apical localization (A and B). In pseudohyphal-promoting conditions, the *bem3*Δ/Δ *rga2*Δ/Δ *MLC1-YFP* strain displays a Spitzenkörper shown by the apical spot of Mlc1-YFP fluorescence (C–E) that colocalizes with FM4-64 (E). Mutants lacking one of the Cdc42 GAPs and the triple *bem3*Δ/Δ *rga2*Δ/Δ *rdi1*Δ/Δ mutant also display a Spitzenkörper in a high proportion of cells (F–H). At later times in the *bem3*Δ/Δ *rga2*Δ/Δ strain, Mlc1-YFP simultaneously localizes to a Spitzenkörper at the tip and to a cytokinetic ring within the germ tube (I). Unbudded yeast cells of the indicated genotype were reinoculated into conditions that promote pseudohyphal growth (A–I) or hyphal growth (J). (A–H) Samples were withdrawn 70 min after induction. (I) Samples withdrawn 110 min after induction. Cells in A–D, F–H, and I are counterstained with concanavalin A–Texas-Red added 5 min before sampling; note the mother cells stain poorly with this reagent. Cells in E are counterstained with calcofluor white added 5 min before sampling. B and C show expanded views of the arrowed cells in A and D, respectively. All images are of unfixed cells. Bars, 5 μm except I, 10 μm. HF, growth in conditions that promote the hyphal form; PH, growth in conditions that normally promote pseudohyphal growth.

neck in parental BWP17 cells, compared with *bem3*Δ/Δ *rga2*Δ/Δ cells (Figure 7C). Thus, *bem3*Δ/Δ *rga2*Δ/Δ cells growing in pseudohyphal conditions show the hyphal pattern of nuclear division.

Rga2 and Bem3 Function Is GAP Dependent

To investigate whether the role of Rga2 and Bem3 requires their GAP activity or whether their role is GAP independent, we constructed strains carrying point mutations in the GAP genes that specifically target GAP activity. Two classes of mutation were generated. First, a highly conserved lysine in the GAP domain was replaced by alanine to create *rga2*^{K1061} and *bem3*^{K1025A}. These mutations are equivalent to *rga1*^{K872A} in *S. cerevisiae* that has been shown to both destroy GAP activity and to prevent the interaction between Rga1 and Cdc42 (Gladfelter *et al.*, 2002). Additionally, the analogous p190GD^{K1321A} mutant of the human Rho-GAP failed to bind to or stimulate the GTPase activity of RhoA (Li *et al.*, 1997). The second class of mutation was the replacement of a conserved arginine that protrudes into the active site of the Rho-GTPase and is thought to stabilize the transition state of the GTPase reaction (Rittinger *et al.*, 1997). In the human Cdc42-GAP, replacement of this arginine by alanine (Cdc42hs-GAP^{R305A}) greatly reduced the catalytic activity of Cdc42-GAP without affecting its affinity for Cdc42hs (Leonard *et al.*, 1998). Similarly, the p190GD^{R1283L} protein lost GAP activity but retained affinity for RhoA (Li *et al.*, 1997). The equivalent mutations in the *C. albicans* GAP genes are *rga2*^{R1015L} and *bem3*^{R985L}. We replaced the critical arginine residue with leucine, because the alanine substitution in Cdc42hs-GAP^{R305A} resulted in a protein with detectable GAP activity.

Strains were constructed in which a GAP gene carrying one of these point mutations was the sole copy of one or other of the GAP genes (e.g., *BEM3/BEM3 rga2*Δ/*rga2*^{R1015L}) or in which the mutant gene was the only copy of either GAP gene (e.g., *bem3*Δ/Δ *rga2*Δ/*rga2*^{R1015L}). A list of the strains constructed is listed in Table 2, which also shows data describing the morphology of the strains growing under pseudohyphal-promoting conditions and the percentage of cells in which the septa formed away from the bud neck. It was necessary to monitor the position of the septa using calcofluor white staining rather than the position of the septin ring, because the process of strain construction resulted in strains with no markers with which to introduce Cdc10-YFP fusions. We have previously shown that the septa forms at the site of the septin ring (Sudbery, 2001). In every case, the point mutation had exactly the same effect as the equivalent deletion allele (Table 2). For example, the *rga2*Δ/*rga2*^{R1015L} and *rga2*Δ/*rga2*^{K1061A} strains showed a similar degree of enhanced polarized growth as the *rga2*Δ/Δ strain; and the *bem3*Δ/Δ *rga2*Δ/*rga2*^{R1015L} and *bem3*Δ/Δ *rga2*Δ/*rga2*^{K1061A} strains showed a similar degree of polarized growth to the *bem3*Δ/Δ *rga2*Δ/Δ strain. Similarly, although the septa predominantly localized to the bud neck in strains that retained a single wild-type copy of either *RGA2* or *BEM3*, it localized within the germ tube/elongated bud in strains in which the only remaining GAP gene carried one of the point mutations (*bem3*Δ/Δ *rga2*Δ/*rga2*^{R1015L}, *bem3*Δ/Δ *rga2*Δ/*rga2*^{K1061A}, *rga2*Δ/Δ *bem3*Δ/*bem3*^{R985L}, and *rga2*Δ/Δ *bem3*Δ/*bem3*^{K1025A}). Thus, the mutant phenotypes arising from loss of the Cdc42 GAP-encoding genes are due to loss of their GTPase-activating function.

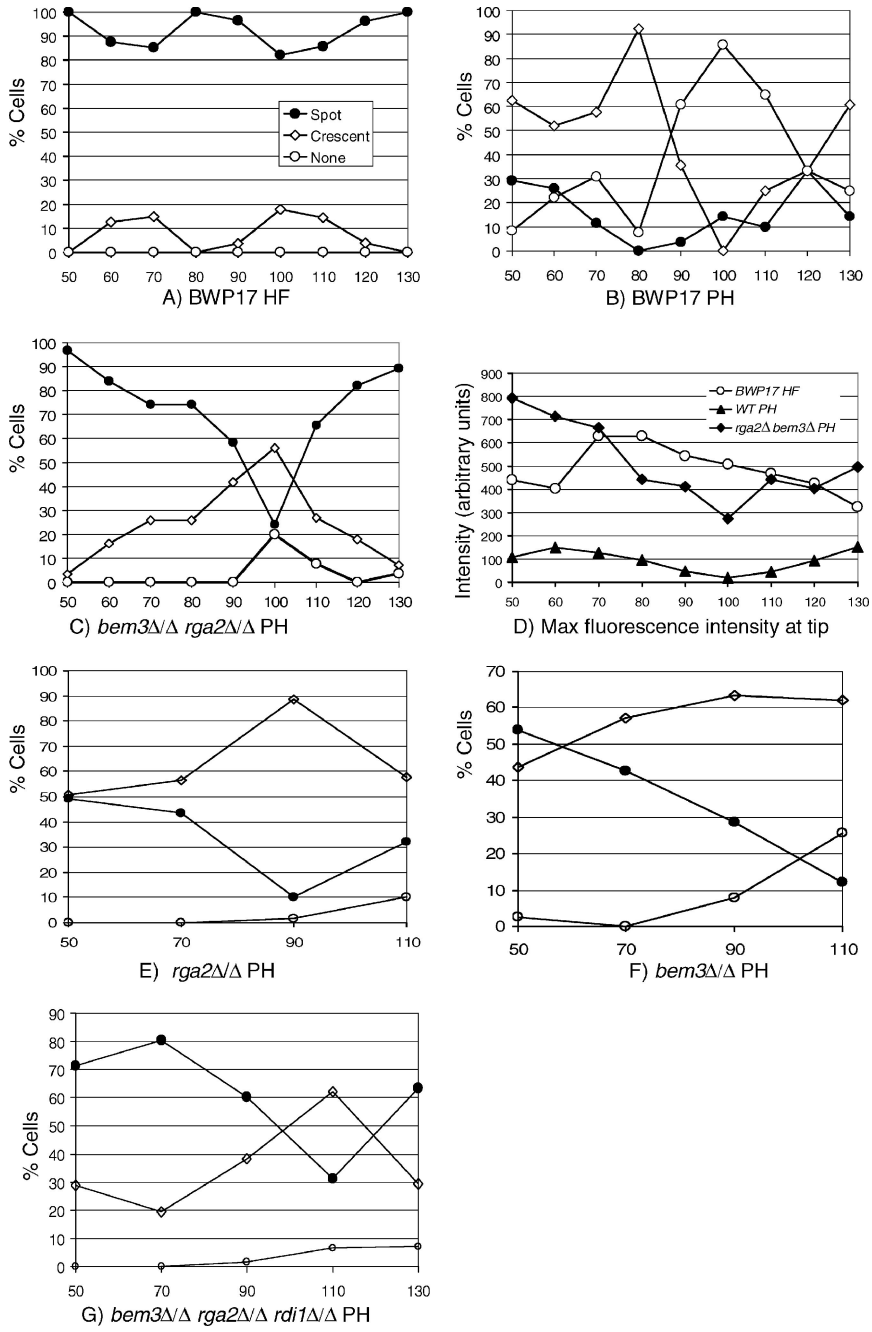

Figure 5. Quantification of Spitzenkörper formation in mutants lacking the Cdc42 GAPs growing under pseudohyphal conditions. (A) Parental BWP17 cells growing as hyphae display an Mlc1-YFP spot at the tip at all times of the cell cycle. The small proportion of cells showing a crescent are probably the 10–15% of cells that grow as pseudohyphae in these conditions (Sudbery, 2001). (B) BWP17 pseudohyphal cells display a crescent of Mlc1-YFP at early times, but all fluorescence disappears completely toward the end of the first cell cycle and reappears at the start of the next cell cycle. (C) Cells lacking the Cdc42 GAPs show a spot at early times that changes to a crescent late in the cell cycle, but in most cells some Mlc1-YFP fluorescence is maintained throughout, and at the start of the next cycle most cells display a spot again. (D) Quantification of peak Mlc1-YFP fluorescence intensity at the tip shows that wild-type hyphae and cells lacking the Cdc42 GAPs show a similar intensity that is three- to fourfold greater than the intensity in pseudohyphal cells. *rga2*Δ/Δ cells (E) and *bem3*Δ/Δ cells (F) growing under pseudohyphal-promoting conditions also display a spot at early times, although these disappear at late times in the cycle, they are replaced by a crescent so that most cells retain some apical localization throughout the cycle. (G) Loss of Rdi1 does not affect the proportion of cells displaying a Spitzenkörper (compare with C). Unbudded cells of the indicated genotype were reinoculated into YEPD to induce pseudohyphal growth (B, C, and E–G) or hyphal growth (A). Samples were withdrawn at intervals and Mlc1-YFP fluorescence imaged in live cells. The pattern of fluorescence was categorized as spot, crescent, or none. In addition the peak intensity of Mlc1, fluorescence was measured in parental hyphae and pseudohyphae and *bem3*Δ/Δ *rga2*Δ/Δ cells growing in pseudohyphal conditions (D). At each time point, 25 cells were analyzed. Except in D, the key for all panels is shown in A. The abscissae on all graphs are minutes after inoculation of unbudded yeast cells. The values of the peak fluorescence intensity for spot, crescent, and none, respectively, were as follows: BWP17 hyphae (A): 538 ± 39, 168 ± 25, not applicable (all hyphae had some Mlc1-YFP fluorescence); BWP17 pseudohyphae (B): 194 ± 43, 75 ± 14, 37 ± 17; and *bem3*Δ/Δ *rga2*Δ/Δ *MLC1-YFP* (C): 656 ± 52, 289 ± 66, 84 ± 16. HF, hyphal form; PH, pseudohyphae.

Expression of a Constitutively GTP-bound Cdc42 Allele Does Not Result in the Same Phenotype as Loss of GAP Function

Deletion of the Cdc42 GAPs is predicted to result in an increased level of Cdc42-GTP, which would be expected to produce a similar phenotype to expression of the constitutively GTP bound $Cdc42^{G12V}$. Previously, it has been that shown that expression of $Cdc42^{G12V}$ from the *PCK1* promoter in *C. albicans* resulted in the formation of aberrant multibudded cells under yeast-inducing conditions, and cells with large, aberrant, branched structures under hyphal-inducing conditions (Ushinsky *et al.*, 2002). However, the effect of expression of $Cdc42^{G12V}$ under pseudohyphal-inducing conditions was not investigated. To investigate whether expression of $Cdc42^{G12V}$ also causes the formation of hyphal characteristics under pseudohyphal conditions, cells of strain CaSU64 (*CDC42*/P_{PCK1}-$CDC42^{G12V}$) (Ushinsky *et al.*, 2002) were grown in YPD medium to saturation overnight in conditions that promote yeast-form growth. The resulting unbudded yeast cells were then reinoculated into culture conditions that normally induce pseudohyphal growth and activation of the *PCK1* promoter (2% casamino acids, 35°C, pH 5.0). The appearance of such cells, along with a parental control, is shown in Figure 8, A and B. Cells expressing $Cdc42^{G12V}$ were swollen, and the mother bud necks were abnormally large. Interestingly, some of the buds showed tip splitting and branching. Thus, in contrast to loss of Cdc42 GAPs, a predicted increase in the level of Cdc42-GTP by expression of $Cdc42^{G12V}$ does not result in a hyphal like morphology.

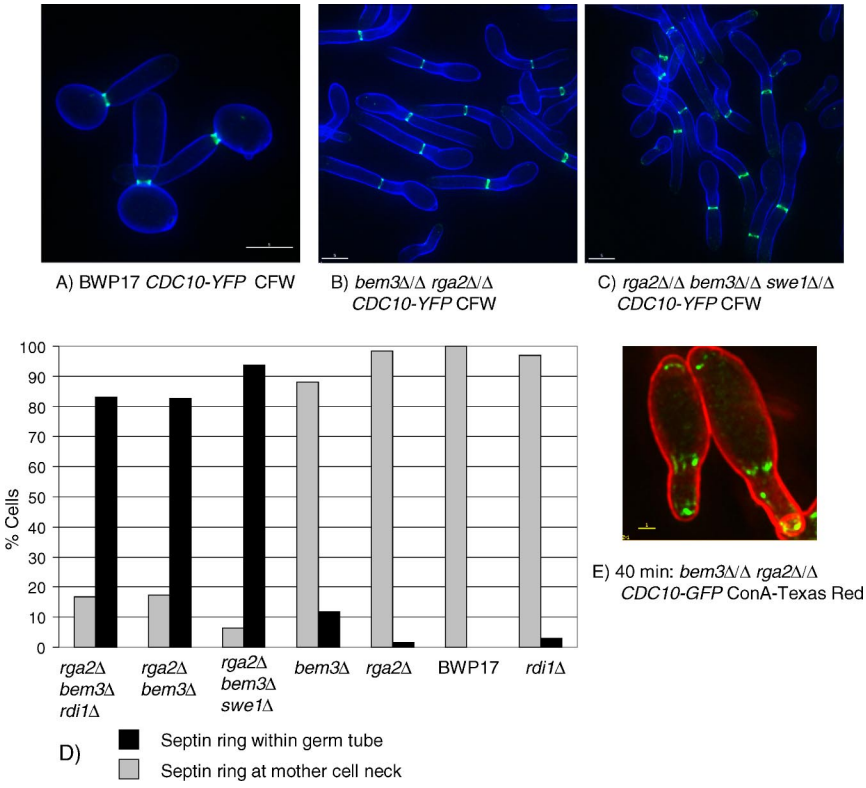

Figure 6. Cdc42 GAPs regulate the location of the septin rings and formation of basal septin bands and caps. When grown pseudohyphal-inducing conditions the septin ring in parental BWP17 cells forms at the mother bud neck (A and D), whereas it forms within the germ tube in *bem3*Δ/Δ *rga2*Δ/Δ cells (B and D) in a Swe1-independent (C and D) and Rdi1-independent manner (D). Shortly after evagination a basal septin band, consisting of longitudinal bars, and an apical septin cap are visible in *bem3*Δ/Δ *rga2*Δ/Δ cells (E). Unbudded cells of the indicated genotypes were reinoculated into pseudohyphal-promoting conditions (pH 6.0, 36°C). Images in A–C and F were recorded in live cells 100 min after reinoculation; the image in D was recorded 40 min after evagination. (A–C) Cells counterstained with calcofluor white (CFW). (E) Cells counterstained with concanavalin A conjugated to Texas-Red (ConA Texas Red). For the quantification shown in D, cells were sampled after 100 min, and 100 cells analyzed for each genotype. Note for clarity in D, the full diploid genotype is not written out; all indicated deletions are homozygous. Bars, 5 μm (A–C) and 1 μm (E).

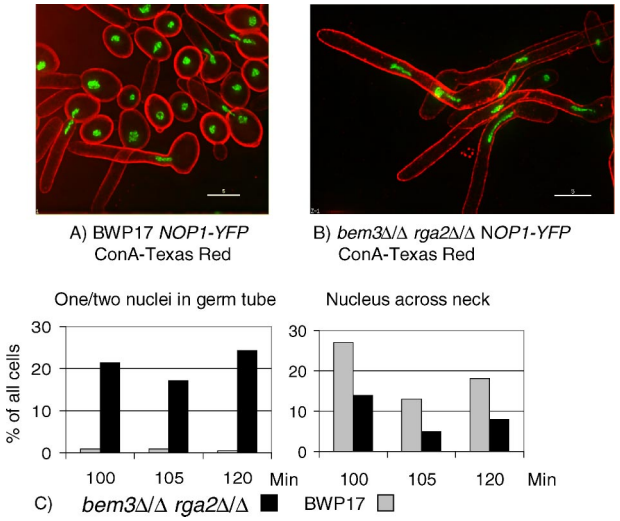

Figure 7. Nuclei migrate into the germ tube in mutants lacking the Cdc42 GAPs growing under pseudohyphal conditions. Nuclei visualized by a *NOP1-YFP* fusion divide across the bud neck in parental cells (A) but migrate into the germ tube in cells lacking the Cdc42 GAPs (B). Images were recorded 100 min after inoculation of stationary phase cells into fresh YEPD medium, pH 6.0, 36°C. The cells shown were fixed and stained with concanavalin A–Texas-Red. Bars, 5 μm. At the indicated time points, cells were monitored for nuclear position (C). Each bar shows the percentage of all cells counted that show the indicated nuclear position. Total cells counted for each strain for the 100-, 105-, and 120-min time points, respectively, are as follows. BWP17: 204, 218, and 183 and *bem3*Δ/Δ *rga2*Δ/Δ: 51, 35, and 66.

To investigate the effect $Cdc42^{G12V}$ expression on Spitzenkörper formation and septin organization, we introduced Mlc1-YFP or Cdc10-YFP fusions, respectively, into CaSU64. The resulting strains were then grown in culture conditions that promote pseudohyphal growth and activation of the *PCK1* promoter as described above. Cdc10-YFP formed a septin ring of normal appearance at the mother bud neck during the first cell cycle after inoculation. However, abnormal striated septin structures formed at the junction between the first and second daughter cells (Figure 8, C and D). Thus, unlike the loss of the Cdc42 GAP proteins, expression of $Cdc42^{G12V}$ does not result in the formation of ectopic septin rings, but it does result the formation of septin bars resembling the basal septin bands of hyphal germ tubes. Consistent with the lack of hyphal-like morphology, Mlc1-YFP localized, if at all, to surface crescents rather than Spitzenkörpers (Figure 8E).

Bem3 Localizes to the Tips of Hyphae and Young Buds; Rga2 Localizes to the Sites of Cytokinesis in Yeast and Pseudohyphae

We next investigated the localization of Rga2, Bem3, and Rdi1 by constructing fusions to YFP. The phenotype of *bem3*Δ/Δ *rga2*Δ */RGA2-YFP* and *rga2*Δ/Δ *bem3*Δ/*BEM3*-YFP were the same as the *bem3*Δ/Δ and *rga2*Δ/Δ strains, respectively, showing that the fusions were functional (data not shown). We observed that Bem3-YFP localized to a bright patch at the tips of hyphae (Figure 9A). However, the morphology was different from the discrete Mlc1-YFP spot that characterizes the Spitzenkörper; rather Bem3-YFP fluorescence formed a more diffuse pattern, which in some hyphal tips seemed to consist of a circle surrounding a nonfluorescing center (Figure 9, B and C). So, Bem3 may not be a Spitzenkörper component. Bem3-YFP also localized to a crescent at the tips of young yeast buds (Figure 9, D and E,),

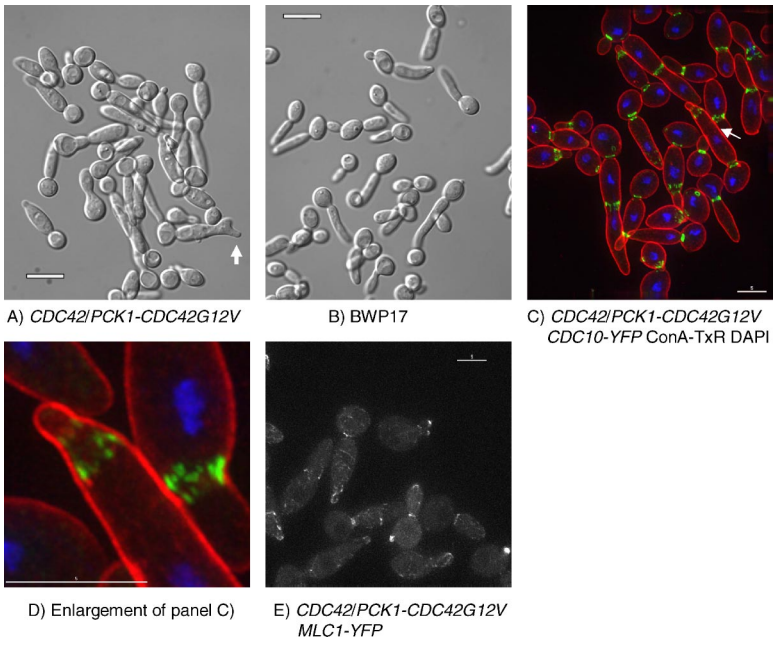

Figure 8. Expression of Cdc42^{G12V} results in loss of polarity and septin bars. (A) Cells expressing Cdc42^{G12V} from the regulatable *PCK1* promoter are swollen and show tip splitting (arrow) compared with parental cells (B). Septin rings form normally in the first cycle after induction, but in the second cycle septins form longitudinal bars rather than rings (C and D). Mlc1-YFP does not localize to apical spots in the majority of cells; in some cells, it forms a faint crescent and in some cells no apical localization is evident (E). Cells of the indicated genotype were grown overnight to stationary phase in YEPD (*CDC*42^{G12V} repressed), washed in distilled water, and reinoculated into media containing 2% Cas amino acids (Difco) 0.67% yeast nitrogen base, 80 mg l^{-1} uridine, pH 5.0, 35°C (pseudohyphal-inducing conditions, *CDC*42^{G12V} induced). Images were recorded after 150 min. Arrow in C indicates cells enlarged in D. Bars, 10 μm (A and B) and 5 μm (C–E). The cells shown in C and D were fixed and stained with concanavalin A–Texas-Red and 4,6-diamidino-2-phenylindole (DAPI). The cells shown in E are unfixed.

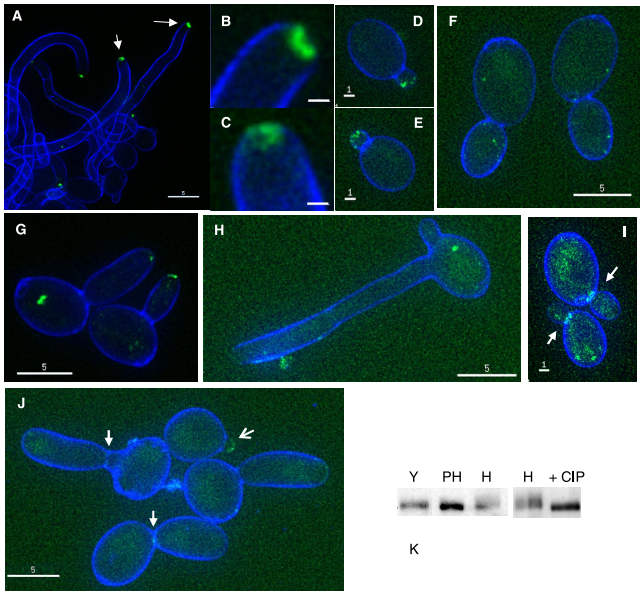

Figure 9. Localization of Bem3-YFP and Rga2-YFP. Bem3-YFP localizes to hyphal tips (A–C), the tips of small yeast buds (D and E), but not large yeast buds (F) and to the tips of pseudohyphal buds (G). Arrows in A indicate the tips shown in detail in B and C. Rga2-YFP is not present at hyphal tips (H) but is present at the sites of septation in yeast (arrows, I) and pseudohyphae (solid arrows, J), and to the tips of young buds (barbed arrow, J). Rga2 is phosphorylated in hyphae but not in yeast or pseudohyphae (K). Stationary phase yeast cells were reinoculated into fresh SD medium and grown as hyphae (A–C and H), pseudohyphae (G and J), or yeast (D–F and I). Cells were counterstained with calcofluor white added 5 min before sampling, and examined with a Delta Vision microscope. Bars, 5 μm (A, F–H, and J), 1 μm (D, E, and I), and 0.5 μm (B and C). (K) Rga2-YFP detected in a Western by anti-GFP mAb (Roche Biosciences). CIP, calf intestinal phosphatase; H, hyphae; PH, pseudohyphae; and Y, yeast.

which disappeared as the bud increased in size (Figure 9F). Bem3-YFP also localized to the tips of pseudohyphal buds (Figure 9G). We did not observe any signal from Bem3-YFP at the sites of septation in any of the three growth forms. In striking contrast to Bem3-YFP, Rga2-YFP was not present at hyphal tips even in overexposed images (Figure 9H). However, Rga2-YFP was observed at sites of septation in pseudohyphae and yeast (Figure 9, I and J). A faint signal was observed at the tips of young pseudohyphal buds, which was faint or nonexistent in larger buds (Figure 9J). No signal was apparent at the tips of young yeast buds (Figure 9I). Thus, Bem3 is predominantly associated with the tips of hyphae and buds, whereas Rga2 is predominantly associated with sites of septation. Rdi1-YFP localized throughout the cytoplasm of both the mother cell and germ tube (Supplemental Figure 2).

Rga2 Is Phosphorylated in a Hyphal-specific Manner

The phenotypes of the *bem3*Δ/Δ *rga2*Δ/Δ mutant suggest that Rga2 and Bem3 may play a physiological role in regulating the formation of hyphal characteristics. However, there is no obvious change in the transcript levels of Rga2 and Bem3 during hyphal induction (Nantel *et al.*, 2002). To investigate the possibility that they are regulated by posttranslation modifications such as phosphorylation, we carried out Western blots by using an anti-GFP mAb and lysates from strains expressing Rga2-YFP or Bem3-YFP. Rga2-YFP showed a band shift specifically in hyphal extracts, which disappeared upon treatment with calf intestinal phosphatase (Figure 9K). Thus, Rga2 is phosphorylated in a hyphal-specific manner, which may provide a mechanism for its down-regulation in hyphae. A band shift of Bem3-YFP was not detected (data not shown).

Apical Localization of Cdc42 Is Enhanced in Cells Lacking the Cdc42 GAPs

In *S. cerevisiae*, polarized growth is initiated by the recruitment of Cdc42, initially in a actin-independent manner (Ayscough *et al.*, 1997). However, there is accumulating evidence that Cdc42 may participate in a positive feedback loop so that localization of Cdc42 can be a self-reinforcing

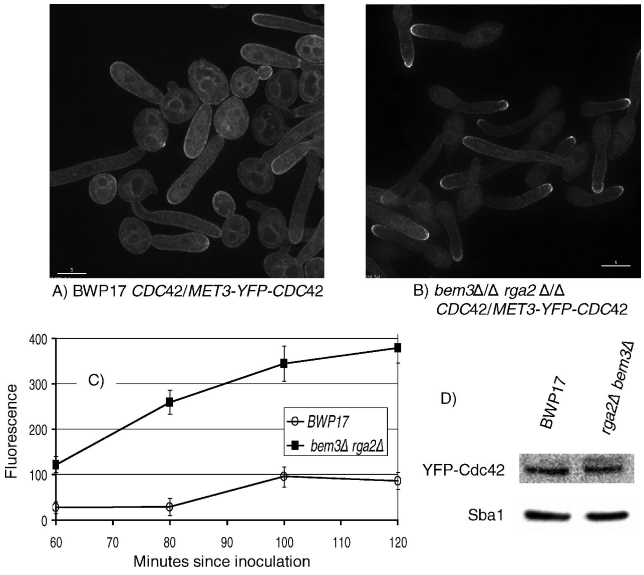

Figure 10. Cdc42 is hyperpolarized in *bem3*Δ/Δ *rga2*Δ/Δ cells growing in pseudohyphal-promoting conditions.YFP-Cdc42 is localized to a bright cap at the tips of *bem3*Δ/Δ *rga2*Δ/Δ cells growing under pseudohyphal conditions. In parental BWP17 cells YFP-Cdc42 is localized to internal membranes and more evenly around the periphery compared with *bem3*Δ/Δ *rga2*Δ/Δ cells. The Western blot shows that the total cellular content of Cdc42 is not significantly different in the two strains. BWP17 *MET3*-YFP-Cdc42 and *MET3*-YFP-Cdc42 *bem3*Δ/Δ *rga2*Δ/Δ cells were grown to stationary phase in YEPD and reinoculated into derepressing SD medium (Wightman *et al*., 2004) at pH 6.0, 36°C. At intervals, samples were withdrawn, and images were recorded with a Delta Vision microscope. The images shown in A and B were recorded 100 min after inoculation. Bars, 5 μm. (C) Peak fluorescence plotted against time. Between 30 and 80 cells were monitored at each time point. Error bars are 95% confidence limits. (D) Western blot using anti-GFP mAb. Anti-Sba1 polyclonal antisera was used as a loading control (see *Materials and Methods*).

process (Zajac *et al*., 2005; Roumanie *et al*., 2005). If this is the case in *C. albicans*, then cells with increased Cdc42 activity, because of the loss of the Cdc42 GAPs, will show increased amounts of Cdc42 at sites of polarized growth. To test this hypothesis, we expressed *YFP-CDC42* from the *MET3* promoter (*MET3-YFP-CDC42*) in parental BWP17 and *bem3*Δ/Δ *rga2*Δ/Δ cells growing in derepressing pseudohyphal conditions (SD medium, pH 6.0, 36°C) and took samples at intervals for imaging. We observed an increase in the brightness of the apical Cdc42 crescent in *bem3*Δ/Δ *rga2*Δ/Δ cells compared with BWP17 cells (Figure 10, A and B), which was confirmed by quantification of the peak fluorescence (Figure 10C). This increase in brightness was not due to increased overall cellular levels of YFP-Cdc42 as Western blots by using an anti-GFP antibody showed that total cellular levels remained constant (Figure 10D). However, more YFP-Cdc42 was visible at internal membranes in the parental cells. Thus, polarized Cdc42 localization is promoted by the absence of Cdc42 GAPs.

DISCUSSION

Cdc42 GAPs Control the Appearance of Hyphal-specific Characteristics

In this work, we have sought to establish whether proteins that regulate Cdc42 activity such as Cdc42 GAPs and Rdi1 are involved in regulating the formation of hyphal characteristics. We found that in conditions that normally promote pseudohyphal growth, cells lacking the Cdc42 GAPs Rga2 and Bem3 display characteristics that distinguish hyphae from pseudohyphae. They form Spitzenkörpers and show accompanying hyperpolarized growth. They show the hyphal pattern of septin organization: septin bands and caps are evident in short germ tubes and septin rings form within the germ tubes as they extend their length. Mlc1-YFP persists in the Spitzenkörper at the same time as Mlc1-YFP occurs in the cytokinetic ring. Finally, they show the hyphal pattern of nuclear division—nuclei migrate into the germ tube before dividing. These phenotypes are reminiscent of the *S. cerevisiae rga1*Δ *rga2*Δ *bem3*Δ mutants; but although these *S. cerevisiae* cells are clearly abnormal, the equivalent *C. albicans* mutants lacking Cdc42 GAPs show many characteristics of normal hyphae, suggesting that the GAP genes may play a physiological role in directing developmental pathways to produce the hyphal rather than the pseudohyphal morphology.

The Role of Rga2 and Bem3 Requires Their GAP Function

To investigate whether the role of Rga2 and Bem3 requires their GAP activity, we generated point mutations in their GTPase-activating domains. The mutations were selected from studies of the highly conserved GAP domain of other proteins and in each case have been shown to have the same effect in more than one GAP protein. They were selected to either abolish GAP activity but leave the interaction with Cdc42 unaffected, or to abolish both GAP activity and the interaction with Cdc42. All mutations had the same effect on polarized growth and septin organization as the relevant deletion allele. Thus, it seems likely that the role of Rga2 and Bem3 requires their GAP activity. However, the possibility remains that their role involves additional GAP-independent functions, such as regulating Cdc42 localization.

Specificity of Rga2 and Bem3 Activity

The interpretation of these results is based on the premise that Rga2 and Bem3 are GAPs for Cdc42 but not other Rho-type GTPases. What is the evidence that this is the case? Biochemical and genetic studies in *S. cerevisiae* strongly suggest that ScRga1/2 and ScBem3 do act as GAPs for ScCdc42. First, several independent studies have shown that these proteins have Cdc42-directed GTPase activity in vitro (Zheng *et al*., 1994; Smith *et al*., 2002; Gladfelter *et al*., 2002). Second, two hybrid studies found that Rga1, Rga2, and Bem3 interact with the activated, but not the inactivated form of Cdc42 (Stevenson *et al*., 1995; Smith *et al*., 2002). At least in the case of Rga2, no interaction was detected with other Rho-type GTPases, even in their activated form. Third, overexpression of *RGA1*, *RGA2*, or *BEM3* lowered the restrictive temperature of a *cdc42* temperature-sensitive (ts) mutant, whereas deletion of either of these genes increased the restrictive temperature of a *cdc24* ts mutant (Stevenson *et al*., 1995; Smith *et al*., 2002). The genes identified here as Ca*RGA2* and Ca*BEM3* encode proteins that are far more similar to Sc*Rga*1/2 and Bem3 than they are to any other putative Rho-GAPs in the *C. albicans* genome. Although it is probable that Rga2 and Bem3 have Cdc42-directed GAP activity, is it possible that they are also active against other Rho-type GTPases and that loss of this activity is responsible for the phenotypes observed? In addition to Cdc42, there are four other genes encoding Rho-type GTPases in the *C. albicans* genome: *RHO1*, *RHO3*, *CRL1* (homologous to *ScRHO4*), and *RAC1*. In *S. cerevisiae*, Rho1 has been shown to have multiple functions in cell integrity and other aspects of cell morphogenesis and growth. Bem2, Sac7, and Bag7 have

been shown to be the Rho1-GAPs, and their specific role in each of the separate Rho1 functions has been characterized previously (Schmidt *et al*., 2002). Homologues for Bem2 and Sac7 are present in the *C. albicans* genome. In *S. cerevisiae*, none of these GAPs seem to play a similar role to Rga1/2 or Bem3. Indeed, deletion of *BEM2* has the opposite effect to deletion of the Cdc42 GAPs, resulting in large unbudded, multinucleate cells displaying a loss of polarity (Bender and Pringle, 1991). Furthermore, in the filamentous yeast *Ashbya gossypii*, a *bem2*Δ mutant was defective in hyphal formation, producing swollen hyphae with a complete loss of polarity (Wendland and Philippsen, 2001). There are conflicting reports of whether Bem2 has Cdc42-directed GAP activity in vitro (Zheng *et al*., 1994; Marquitz *et al*., 2002). Although Bem3 does have some Rho1-GAP activity, it is much lower than its Cdc42-GAP activity. In light of these extensive studies of Rho1 function and the role of Rho1-GAPs, it seems unlikely that the phenotype of *C. albicans bem3*Δ/Δ *rga2*Δ/Δ mutants arises from an effect on CaRho1 activity. Similarly, Rho3 and Rho4 act to promote cell integrity in *S. cerevisiae*. Rgd1, for which a homologue exists in the *C. albicans* genome, has been identified as a specific GAP for ScRho3/4 (Doignon *et al*., 1999). Again, it seems unlikely that stimulation of CaRho3/4 activity is responsible for the *C. albicans bem3*Δ/Δ *rga2*Δ/Δ phenotype. However, the situation is less clear in the case of *C. albicans* Rac1. This GTPase is member of the Rac family of GTPases widely distributed among eukaryotes but not represented in the *S. cerevisiae* genome. The function of *C. albicans* Rac1 has recently been studied (Bassilana and Arkowitz, 2006). Unlike cells depleted of Cdc42, a *rac1*Δ/Δ mutant was able to form hyphae normally in response to serum or pH and 37°C incubation temperature; however, hyphal morphogenesis induced by matrix embedded growth was reduced. Our experiments have not ruled out the possibility that Rga2 and Bem3 have Rac1-directed GTPase activity. However, given the known major role of Cdc42 in hyphal morphogenesis and septin organization compared with the apparently minor role of Rac1, and the parallels between the phenotypes of *S. cerevisiae* and *C. albicans* mutants lacking Rga1/2 and Bem3, it is likely that at least a major part of the phenotype of the *bem3*Δ/Δ *rga2*Δ/Δ mutant feeds through Cdc42.

Activated Cdc42-GTP Is Necessary but Not Sufficient for Hyphal Growth

In the course of this work, we confirmed previous observations of the effect of expressing constitutively GTP-bound $Cdc42^{G12V}$ (Ushinsky *et al*., 2002). We found that such cells growing in pseudohyphal-promoting conditions had a swollen appearance, and localization of Mlc1-YFP revealed that a Spitzenkörper did not form, in contrast to the phenotype of the *bem3*Δ/Δ *rga2*Δ/Δ cells. Thus, elevation of activated Cdc42 levels is not sufficient to induce hyphal growth. Why does expression of $Cdc42^{G12V}$ have a different effect from loss of the Cdc42 GAPs? We suggest two explanations for this apparent anomaly. First, in *S. cerevisiae* the activity of $Cdc42^{G12V}$ has been shown to be independent of Cdc24 and so is locked in the GTP-bound state (Gulli *et al*., 2000). However, wild-type Cdc42 has an unusually high rate of intrinsic GTPase activity compared with other GTPases (Zheng *et al*., 1994), so even in the absence of GAPs, Cdc42 will still be cycling between GDP- and GTP-bound states, although the balance will be shifted toward Cdc42-GTP. Therefore, although Cdc42 will be more active in cells lacking Cdc42 GAPs, it will still require activation by Cdc24, which is localized at the bud tips. This will restrict Cdc42 activation to the bud tip, leading to hyperpolarized growth. An additional factor may be that the high levels of Cdc42-GTP establish a positive feedback loop that recruits further Cdc42 to the bud tips, consistent with the higher levels of YFP-Cdc42 at the tips that we observed in the *bem3*Δ/Δ *rga2*Δ/Δ strain. In contrast, $Cdc42^{G12V}$ is active all around the cell periphery leading to isotropic growth. The tip splitting and branching observed may be due to spontaneous feed back loops arising from local stochastic fluctuations in Cdc42 levels. The second explanation is that GTP/GDP cycling may be required for the action of Cdc42 in promoting polarized growth as it is for septin ring organization (Gladfelter *et al*., 2002).

Formation of the Basal Septin Band and Septin Rings in Hyphae

Expression of the $CDC42^{G12V}$ allele also caused an interesting septin phenotype during growth in pseudohyphal-inducing conditions — septin bars formed at the bud neck, similar to those that form at the base of hyphal germ tubes. These only formed in the second cycle after induction; in the first cycle apparently normal rings formed in at a morphologically normal bud neck. We presume that the delay in the appearance of the abnormal phenotype is due the time taken for the $Cdc42^{G12V}$ protein to accumulate to sufficient levels to have an effect. Although we did not measure $Cdc42^{G12V}$ levels after induction, we did follow the increase in YFP-Cdc42 fluorescence after it was expressed from the *MET3* promoter and found that it continued to increase throughout the whole of the 120-min time course (Figure 10C). In contrast, during growth in pseudohyphal conditions the *bem3*Δ/Δ *rga2*Δ/Δ mutant formed apparently normal rings at an ectopic location within a hyphal-like germ tube, although septin bars did form transiently in some cells.

In *S. cerevisiae*, it is thought that formation of a functioning septin structure at the bud neck consists of three stages: recruitment of septin subunits or septin filaments, the formation of a septin ring, in which the subunits are in dynamic equilibrium with the pool of free subunits, and the conversion of the ring to a septin collar in which the subunits are nondynamic (Gladfelter *et al*., 2002; Caviston *et al*., 2003; Dobbelaere *et al*., 2003; Iwase *et al*., 2006). The role of the GAP proteins and GTP hydrolysis in these processes has been the subject of much discussion recently. Studies of the phenotype of the GTP hydrolysis-defective *cdc42* alleles and the involvement of Cdc42 GAPs support a model in which the formation of the ring depends on cycles of GTP hydrolysis similar to the role of the elongation factor EF-Tu in protein synthesis (Gladfelter *et al*., 2002); however, it has been argued that initial recruitment of septin subunits depends on activated Cdc42-GTP (Iwase *et al*., 2006). Formation of the ring and the stable collar structure also depends on a number of other proteins, including Nap1 and the kinases Gin4 and Cla4. In light of this model, we interpret the different phenotypes of the strain expressing $Cdc42^{G12V}$ and the *bem3*Δ/Δ *rga2*Δ/Δ strain as follows. In the former mutant, Cdc42 is locked in the active GTP-bound conformation. This promotes excessive recruitment of septin subunits, but the complete absence of GTP hydrolysis prevents the maturation of these subunits into a ring, resulting in the septin bars observed. In the case of the *bem3*Δ/Δ *rga2*Δ/Δ mutant, the GTP hydrolysis rate of Cdc42 should be reduced due to the absence of GAPs, but some intrinsic GTPase activity would be expected to remain. Initially, the increased levels of Cdc42-GTP results in the recruitment of septin subunits without their onward maturation into a ring, so that septin bars form at the base of the polarized bud or germ tube. However, the residual intrinsic GTPase activity

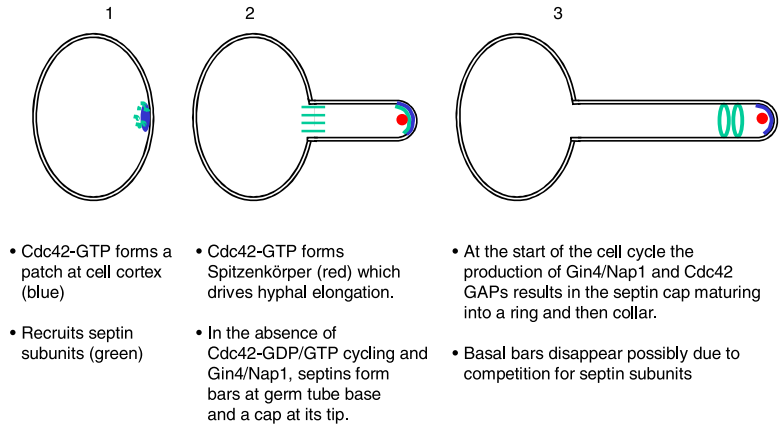

Figure 11. Model for the role of Cdc42 regulation in hyphal formation.

of Cdc42 eventually allows rings to form within the elongating bud.

A Model for Germ Tube Formation

The septin bars that form upon expression of $Cdc42^{G12V}$, the basal septin bars in a germ tube, and the septin phenotype of *S. cerevisiae gin4*Δ mutants show a striking similarity to each other. We have shown that in *C. albicans* germ tubes, formation of septin rings, but not the basal septin band, is dependent on Gin4 (Wightman *et al.*, 2004) and Nap1 (Chapa-y-Lazo and Sudbery, unpublished data). We propose the following model of *C. albicans* germ tube formation (Figure 11). Signal transduction pathways responding to environmental cues lead to a local concentration of Cdc42-GTP at the cortex of G_1 cells. The mechanism for this is currently unclear, but it probably involves activated Ras-GTPase. Cdc42-GTP recruits septin subunits. However, Gin4 is not present in stationary phase *C. albicans* cells (Wightman *et al.*, 2004), and it is also possible that GAP-stimulated Cdc42 GTP/GDP cycling is not occurring; so maturation of these subunits to septin rings is blocked resulting in septin bars. Activated Cdc42-GTP also induces Spitzenkörper formation and hyperpolarized growth. However, the absence of a septin ring at the neck prevents the formation of the constriction normally found in yeast and pseudohyphae (Gladfelter *et al.*, 2005). Cell cycle initiation results in the expression of Gin4 and Nap1, which allows the maturation of the septin subunits into the ring and subsequently the collar structure, which seem to form from the septin cap at the germ tube tip. Consistent with this hypothesis, it has been recently shown that the appearance of the septin ring within the germ tube is coincident with spindle pole body duplication, which marks the start of the cell cycle (Finley and Berman, 2005). Note, however, that these septin rings do not result in a constriction, so their properties differ in some way from the rings at the bud neck of yeast and pseudohyphae. Maintenance of hyphal growth requires that activated Cdc42 is restricted to the germ tube tip and this involves components of the bud selection pathway such as Rsr1 and Bud2, because in the absence of these proteins polarized growth is not continuous and the Spitzenkörper is not maintained in a fixed position at the apex (Bassilana *et al.*, 2003; Hausauer *et al.*, 2005). We note that many of these characteristics are also shown by *S. cerevisiae* mating projections, which are also initiated in the absence of cell cycle progression, suggesting that a similar mechanism may be operating.

Rdi1 Is Not Simply a Negative Regulator of Cdc42

Another potential regulator of Cdc42 is Rdi1, which would be expected to maintain Cdc42 in its inactive GDP-bound state and reduce its membrane association required for activity. Unexpectedly, we found that Rdi1 acts as a positive regulator of polarized growth as *bem3*Δ/Δ *rga2*Δ/Δ *rdi1*Δ/Δ mutants were less polarized than *bem3*Δ/Δ *rga2*Δ/Δ cells. The protein identified as CaRdi1 is highly conserved showing strong similarity not only to the Rdi1 homologues of other fungi, but also to the human Rho-guanine dissociation inhibitor (Supplemental Figure 3). Thus, it is highly likely that we have identified the *C. albicans* Rdi1 homologue. Furthermore, we confirmed that Rdi1 physically associates with Cdc42. However, this does not rule out the possibility that it acts on other Rho-GTPases such as Rho1. Loss of the Rho1-GAP, Bem2, leads to a loss of polarization in *S. cerevisiae* and *A. gossypii* (Bender and Pringle, 1991; Wendland and Philippsen, 2000). Because loss of Rdi1 is expected to have a similar effect on Rho1 activity, this may be the explanation for the reduced polarity we observed. An alternative possibility is that Rdi1 acts to remove Cdc42 from the membrane at sites just behind the growing tip, thus ensuring that the only active Cdc42 is at the growing tip.

Swe1 Is Not Required for the Hyphal Pattern of Septin Ring Formation in Mutants That Lack Cdc42, but It Does Play a Role in Filamentation

Gladfelter *et al.* (2005) found that the formation of ectopic septin rings in $Cdc42^{V36T\ K94E}$ mutants of *S. cerevisiae* was Swe1 dependent. Furthermore, overexpression of Swe1 not only exacerbated the defects in septin organization and localization in $cdc42^{V36T\ K94E}$ mutants but also in mutants of a number of other cell cycle effectors, some of which had not previously been associated with septin defects. They concluded that factors such as Cdc42 that promote septin ring and patch formation in G_1 are dispersed upon activation of the Clb2/Cdc28 kinase in G_2. However, Caviston *et al.* (2003) reported that in *S. cerevisiae* mutants lacking a Cdc42 GAP, deletion of Swe1 did not affect the ectopic formation of septin rings. We also found that a *swe1*Δ/Δ mutation had no discernible effect on the position of the septin ring in the double *bem3*Δ/Δ *rga2*Δ/Δ mutant. This is consistent with our previous observation that formation of hyphal germ tubes, including the pattern of septin ring formation, is normal in a *swe1*Δ/Δ mutant (Wightman *et al.*, 2004). Unexpectedly, we observed that the *swe1*Δ/Δ mutation abolished filamentation on Spider medium. Thus, although the formation of hyphal germ tubes is not Swe1 dependent, Swe1 does

seem to play a role in the long-term maintenance of a filamentous state on Spider medium. In this respect, the *swe1*Δ/Δ allele has a similar effect to a number of other mutations that allow the establishment of germ tube formation in liquid culture but that are defective in the long-term maintenance of the hyphal state, so that colonies are not filamentous when grown on the surface of solid Spider medium or other media that induce filamentous growth. These mutations include *pld1*Δ/Δ, a phosphatidyl choline-specific phospholipase D1 (Hube *et al*., 2001); Cph1, the *C. albicans* homolog of the *S. cerevisiae* Ste12 transcription factor targeted by the pheromone response pathway (Liu *et al*., 1994); and Cln1, which is a G_1 cyclin (now renamed Ccn1) (Loeb *et al*., 1999). These mutations suggest that the establishment of polarized growth in germ tubes growth requires different functions from the long-term maintenance of the filamentous growth.

Rga2 and Bem3 Show Different Patterns of Localization

The phenotypes of the mutants described here suggest that Rga2 and Bem3 are each involved in regulating both polarized growth and septin ring localization. So they might be expected to show similar patterns of localization. However, localization of Bem3-YFP was shown to be primarily apical, whereas Rga2-YFP primarily localized to sites of septation. It is possible that our methods were insufficiently sensitive to detect low levels of localization. For example, some Rga2 may be apically localized; indeed we did observe some localization of Rga2-YFP at the tips of pseudohyphae. A precedent for this situation in *S. cerevisiae* is the way in which the formins Bnr1 and Bni1 share at least some overlapping functions in polarized growth and septin ring formation, because they are functionally redundant; yet, Bni1 primarily localizes to bud tips and Bnr1 to the bud neck (Evangelista, 1997; Kamei *et al*., 1998).

Rga2 Is Phosphorylated in a Hyphal-specific Manner

Rga2 was found to be phosphorylated in a hyphal-specific manner. This observation suggests that a possible mechanism for the initiation of hyphal formation may be the phosphorylation of Rga2, resulting in a decrease of its activity and/or change in its pattern of localization. If this is the case, then the kinase responsible will form the next step in a pathway that might ultimately be targeted by the well-known signal transduction pathways that respond to environmental cues to initiate hyphal growth.

ACKNOWLEDGMENTS

We are grateful to the Berman, Gale, Mitchell, and Whiteway laboratories for strains and plasmids and to the Piper laboratory for the Sba1 polyclonal antisera. We thank Bernardo Chapa-y-Lazo and Mehdi Mollapour for critical reading of the manuscript. This work was supported by a research project grant from the Biotechnology and Biological Sciences Research Council (BB/C514566/1). H.C. was in receipt of a research training studentship from the Medical Research Council.

REFERENCES

Adams, A., Johnson, D., Longnecker, R., Sloat, B., and Pringle, J. (1990). CDC42 and CDC43, two additional genes involved in budding and the establishment of cell polarity in the yeast *Saccharomyces cerevisiae*. J. Cell Biol. *111*, 131–142.

Ayscough, K. R., Stryker, J., Pokala, N., Sanders, M., Crews, P., and Drubin, D. G. (1997). High rates of actin filament turnover in budding yeast and roles for actin in establishment and maintenance of cell polarity revealed using the actin inhibitor latrunculin-A. J. Cell Biol. *137*, 399–416.

Bartnicki-Garcia, S., Hergert, F., and Gierz, G. (1989). Computer-simulation of fungal morphogenesis and the mathematical basis for hyphal (tip) growth. Protoplasma *153*, 46–57.

Bassilana, M., and Arkowitz, R. A. (2006). Rac1 and Cdc42 have different roles in *Candida albicans* development. Eukaryot. Cell *5*, 321–329.

Bassilana, M., Blyth, J., and Arkowitz, R. A. (2003). Cdc24, the GDP-GTP exchange factor for Cdc42, is required for invasive hyphal growth of *Candida albicans*. Eukaryot. Cell *2*, 9–18.

Beck-Sague, C. M., and Jarvis, W. R. (1993). National nosecomial infections surveillance system. Secular trends in the epidemiology of nosocomial fungal infections in the United States 1980–1990. J. Infect. Dis. *167*, 1247–1251.

Bender, A., and Pringle, J. R. (1991). Use of a screen for synthetic lethal and multicopy suppressee mutants to identify two new genes involved in morphogenesis in *Saccharomyces cerevisiae*. Mol. Cell Biol. *11*, 1295–1305.

Berman, J., and Sudbery, P. E. (2002). *Candida albicans*: a molecular revolution built on lessons from budding yeast. Nat. Rev. Genet. *3*, 918–930.

Brand, A., MacCallum, D. M., Brown, A.J.P., Gow, N.A.R., and Odds, F. C. (2004). Ectopic expression of *URA*3 can influence the virulence phenotypes and proteome of *Candida albicans* but can be overcome by targeted reintegration of *URA3* at the *RPS*10 locus. Eukaryot. Cell *3*, 900–909.

Braun, B. R., *et al*. (2005). A human-curated annotation of the *Candida albicans* genome. PLoS Genet. *1*, 36–57.

Bretscher, A. (2003). Polarized growth and organelle segregation in yeast: the tracks, motors, and receptors. J. Cell Biol. *160*, 811–816.

Care, R. A., Trevethick, J., Binley, K. M., and Sudbery, P. E. (1999). The *MET3* promoter: a new tool for *Candida albicans* molecular genetics. Mol. Microbiol. *34*, 792–798.

Caviston, J. P., Longtine, M., Pringle, J. R., and Bi, E. (2003). The role of Cdc42p GTPase-activating proteins in assembly of the septin ring in yeast. Mol. Biol. Cell *14*, 4051–4066.

Crampin, H., Finley, K., Gerami-Nejad, M., Court, H., Gale, C., Berman, J., and Sudbery, P. E. (2005). *Candida albicans* hyphae have a Spitzenkörper that is distinct from the polarisome found in yeast and pseudohyphae. J. Cell Sci. *118*, 2935–2947.

DerMardirossian, C., and Bokoch, G. M. (2005). GDIs: central regulatory molecules in Rho GTPase activation. Trends Cell Biol. *15*, 356–363.

Dobbelaere, J., Gentry, M. S., Hallberg, R. L., and Barral, Y. (2003). Phosphorylation-dependent regulation of septin dynamics during the cell cycle. Dev. Cell *4*, 345–357.

Doignon, F., Weinachter, C., Roumanie, O., and Crouzet, M. (1999). The yeast Rgd1p is a GTPase activating protein of the Rho3 and Rho4 proteins. FEBS Lett. *459*, 458–462.

Evangelista, M. (1997). Bni1p, a yeast formin linking Cdc42p and the actin cytoskeleton during polarized morphogenesis. Science *276*, 118–121.

Evangelista, M., Pruyne, D., Amberg, D. C., Boone, C., and Bretscher, A. (2002). Formins direct Arp2/3-independent actin filament assembly to polarize cell growth in yeast. Nat. Cell Biol. *4*, 32–41.

Finley, K. R., and Berman, J. (2005). Microtubules in *Candida albicans* hyphae drive nuclear dynamics and connect cell cycle progression to morphogenesis. Eukaryot. Cell *4*, 1697–1711.

Fischer-Parton, S., Parton, R. M., Hickey, P. C., Dijksterhuis, J., Atkinson, H. A., and Read, N. D. (2000). Confocal microscopy of FM4-64 as a tool for analysing endocytosis and vesicle trafficking in living fungal hyphae. J. Microsc. *198*, 246–259.

Gerami-Nejad, M., Berman, J., and Gale, C. (2001). Cassettes for PCR-mediated construction of green, yellow and cyan fluorescent protein fusions in *Candida albicans*. Yeast *18*, 859–880.

Gerami-Nejad, M., Hausauer, D., McClellan, M., Berman, J., and Gale, C. (2004). Cassettes for the PCR-mediated construction of regulatable alleles in *Candida albicans*. Yeast *21*, 429–436.

Gladfelter, A. S., Bose, I., Zyla, T. R., Bardes, E.S.G., and Lew, D. J. (2002). Septin ring assembly involves cycles of GTP loading and hydrolysis by Cdc42p. J. Cell Biol. *156*, 315–326.

Gladfelter, A. S., Kozubowski, L., Zyla, T. R., and Lew, D. J. (2005). Interplay between septin organization, cell cycle and cell shape in yeast. J. Cell Sci. *118*, 1617–1628.

Gola, S., Martin, R., Walther, A., Dunkler, A., and Wendland, J. (2003). New modules for PCR-based gene targeting in *Candida albicans*: rapid and efficient gene targeting using 100 bp of flanking homology region. Yeast *20*, 1339–1347.

Gulli, M. P., Jaquenoud, M., Shimada, Y., Niederhauser, G., Wiget, P., and Peter, M. (2000). Phosphorylation of the Cdc42 exchange factor Cdc24 by the PAK-like kinase Cla4 may regulate polarized growth in yeast. Mol. Cell *6*, 1155–1167.

Hartwell, L. H. (1974). The *Saccharomyces* cell cycle. Bacteriol. Rev. *38*, 164–198.

Hausauer, D. L., Gerami-Nejad, M., Kistler-Anderson, C., and Gale, C. A. (2005). Hyphal guidance and invasive growth in *Candida albicans* require the Ras-like GTPase Rsr1p and its GTPase-activating protein Bud2p. Eukaryot. Cell *4*, 1273–1286.

Hazan, I., Sepulveda-Becerra, M., and Liu, H. P. (2002). Hyphal elongation is regulated independently of cell cycle in *Candida albican*s. Mol. Biol. Cell *13*, 134–145.

Hube, B., Hess, D., Baker, C. A., Schaller, M., Schafer, W., and Dolan, J. W. (2001). The role and relevance of phospholipase D1 during growth and dimorphism of *Candida albicans*. Microbiology *147*, 879–889.

Iwase, M., Luo, J. Y., Nagaraj, S., Longtine, M., Kim, H. B., Haarer, B. K., Caruso, C., Tong, Z. T., Pringle, J. R., and Bi, E. F. (2006). Role of a Cdc42p effector pathway in recruitment of the yeast septins to the presumptive bud site. Mol. Biol. Cell *17*, 1110–1125.

Johnson, D. I. (1999). Cdc *42*, an essential Rho-type GTPase controlling eukaryotic cell polarity. Microbiol. Mol. Biol. Rev. *63*, 54–105.

Johnson, D. I., and Pringle, J. R. (1990). Molecular characterization of *CDC*42, a *Saccharomyces cerevisiae* gene involved in the development of cell polarity. J. Cell Biol. *111*, 143–152.

Kamei, T., Tanaka, K., Hihara, T., Umikawa, M., Imamura, H., Kikyo, M., Ozaki, K., and Takai, Y. (1998). Interaction of Bnr1p with a novel Src homology 3α domain-containing Hof1p. Implication in cytokinesis in *Saccharomyces cerevisiae*. J. Biol. Chem. *273*, 28341–28345.

Kibbler, C. C., Seaton, S., Barnes, R. A., Gransden, W. R., Holliman, R. E., Johnson, E. M., Perry, J. D., Sullivan, D. J., and Wilson, J. A. (2003). Management and outcome of bloodstream infections due to *Candida* species in England and Wales. J. Hosp. Infect. *54*, 18–24.

Koch, G., Tanaka, K., Masuda, T., Yamochi, W., Nonaka, H., and Takai, Y. (1997). Association of the Rho family small GTP-binding proteins with Rho GDP dissociation inhibitor (Rho GDI) in *Saccharomyces cerevisiae*. Oncogene *15*, 417–422.

Leonard, D. A., Lin, R., Cerione, R. A., and Manor, D. (1998). Biochemical studies of the mechanism of action of the Cdc42-GTPase-activating protein. J. Biol. Chem. *273*, 16210–16215.

Lew, D. J., and Reed, S. I. (1995). A cell-cycle checkpoint monitors cell morphogenesis in budding yeast. J. Cell Biol. *129*, 739–749.

Li, R., Zhang, B., and Zheng, Y. (1997). Structural determinants required for the interaction between Rho GTPase and the GTPase-activating domain of p190. J. Biol. Chem. *272*, 32830–32835.

Liu, H., Kohler, J., and Fink, G. R. (1994). Suppression of hyphal formation in *Candida albicans* by mutation of a *STE12* homolog. Science *266*, 1723–1726.

Loeb, J. J., Sepulveda-Becerra, M., Hazan, I., and Liu, H. P. (1999). A G1 cyclin is necessary for maintenance of filamentous growth in *Candida albicans*. Mol. Cell. Biol. *19*, 4019–4027.

Marquitz, A. R., Harrison, J. C., Bose, I., Zyla, T. R., McMillan, J. N., and Lew, D. J. (2002). The Rho-GAP Bem2p plays a GAP-independent role in the morphogenesis checkpoint. EMBO J. *21*, 4012–4025.

Masuda, T., Tanaka, K., Nonaka, H., Yamochi, W., Maeda, A., and Takai, Y. (1994). Molecular-cloning and characterization of yeast-Rho GDP dissociation inhibitor. J. Biol. Chem. *269*, 19713–19718.

Millson, S. H., Truman, A. W., King, V., Prodromou, C., Pearl, L. H., and Piper, P. W. (2005). A two-hybrid screen of the yeast proteome for Hsp90 interactors uncovers a novel Hsp90 chaperone requirement in the activity of a stress-activated mitogen-activated protein kinase, Slt2p (Mpk1p). Eukaryot. Cell *4*, 849–860.

Nantel, A., *et al*. (2002). Transcription profiling of *Candida albicans* cells undergoing the yeast-to-hyphal transition. Mol. Biol. Cell *13*, 3452–3465.

Pruyne, D., Legesse-Miller, A., Gao, L. N., Dong, Y. Q., and Bretscher, A. (2004). Mechanisms of polarized growth and organelle segregation in yeast. Annu. Rev. Cell Dev. Biol. *20*, 559–591.

Rittinger, K., Walker, P. A., Eccleston, J. F., Smerdon, S. J., and Gamblin, S. J. (1997). Structure at 1.65 A of RhoA and its GTPase-activating protein in complex with a transition-state analogue. Nature *389*, 758–762.

Roumanie, O., Wu, H., Molk, J. N., Rossi, G., Bloom, K., and Brennwald, P. (2005). Rho GTPase regulation of exocytosis in yeast is independent of GTP hydrolysis and polarization of the exocyst complex. J. Cell Biol. *170*, 583–594.

Sagot, I., Rodal, A. A., Moseley, J., Goode, B. L., and Pellman, D. (2002). An actin nucleation mechanism mediated by Bni1 and profilin. Nat. Cell Biol. *4*, 626–631.

Schmidt, A., Schmelzle, T., and Hall, M. N. (2002). The Rho1-GAPs Sac7, Bem2 and Bag7 control distinct Rho1 functions in *Saccharomyces cerevisiae*. Mol. Microbiol. *45*, 1433–1441.

Sheu, Y. J., Santos, B., Fortin, N., Costigan, C., and Snyder, M. (1998). Spa2p interacts with cell polarity proteins and signaling components involved in yeast cell morphogenesis. Mol. Cell. Biol. *18*, 4053–4069.

Smith, G. R., Givan, S. A., Cullen, P., and Sprague, G. F. (2002). GTPase-activating proteins for Cdc42. Eukaryot. Cell *1*, 469–480.

Soll, D. R., Herman, M. A., and Staebell, M. A. (1985). The involvement of cell wall expansion in the two modes of mycelium formation of *Candida albicans*. J. Gen. Microbiol. *131*, 2367–2375.

Stevenson, B. J., Ferguson, B., Devirgilio, C., Bi, E., Pringle, J. R., Ammerer, G., and Sprague, G. F. (1995). Mutation of Rga1, which encodes a putative GTPase-activating protein for the polarity-establishment protein Cdc42p, activates the pheromone-response pathway in the yeast *Saccharomyces cerevisiae*. Gene Dev. *9*, 2949–2963.

Sudbery, P. E. (2001). The germ tubes of *Candida albicans* hyphae and pseudohyphae show different patterns of septin ring localisation. Mol. Microbiol. *41*, 19–31.

Sudbery, P. E., Gow, N.A.R., and Berman, J. (2004). The distinct morphogenic states of *Candida albicans*. Trends Microbiol. *12*, 317–324.

Umeyama, T., Kaneko, A., Nagai, Y., Hanaoka, N., Tanabe, K., Takano, Y., Niimi, M., and Uehara, Y. (2005). *Candida albicans* protein kinase CaHsl1p regulates cell elongation and virulence. Mol. Microbiol. *55*, 381–395.

Ushinsky, S. C., Harcus, D., Ash, J., Dignard, D., Marcil, A., Morchhauser, J., Thomas, D. Y., Whiteway, M., and Leberer, E. (2002). CDC42 is required for polarized growth in the human pathogen *Candida albicans*. Eukaryot. Cell *1*, 95–104.

vandenBerg, A. L., Ibrahim, A. S., Edwards, J. E., Toenjes, K. A., and Johnson, D. I. (2004). Cdc42p GTPase regulates the budded-to-hyphal-form transition and expression of hypha-specific transcripts in *Candida albicans*. Eukaryot. Cell *3*, 724–734.

Virag, A., and Harris, S. D. (2006). The Spitzenkörper: a molecular perspective. Mycol. Res. *110*, 4–13.

Warenda, A. J., and Konopka, J. B. (2002). Septin function in *Candida albicans* morphogenesis. Mol. Biol. Cell *13*, 2732–2746.

Wendland, J., and Philippsen, P. (2001). Cell polarity and hyphal morphogenesis are controlled by multiple Rho-protein modules in the filamentous ascomycete *Ashbya gossypii*. Genetics *157*, 601–610.

Wendland, J., and Philippsen, P. (2000). Determination of cell polarity in germinated spores and hyphal tips of the filamentous ascomycete *Ashbya gossypii* requires a rhoGAP homolog. J. Cell Sci. *113*, 1611–1621.

Wightman, R., Bates, S., Amnorrattapan, P., and Sudbery, P. E. (2004). In *Candida albicans*, the Nim1 kinases Gin4 and Hsl1 negatively regulate pseudohypha formation and Gin4 also controls septin organization. J. Cell Biol. *164*, 581–591.

Wilson, B., Davis, D., and Mitchell, A. P. (1999). Rapid hypothesis testing in *Candida albicans* through gene disruption with short homology regions. J. Bacteriol. *181*, 1868–1874.

Wilson, R. B., Davis, D., Enloe, B. M., and Mitchell, A. P. (2000). A recyclable *Candida albicans URA3* cassette for PCR product-directed gene disruptions. Yeast *16*, 65–70.

Zajac, A., Sun, X. L., Zhang, J., and Guo, W. (2005). Cyclical regulation of the exocyst and cell polarity determinants for polarized cell growth. Mol. Biol. Cell *16*, 1500–1512.

Zheng, Y., Cerione, R., and Bender, A. (1994). Control of the yeast bud-site assembly GTPase Cdc42–catalysis of guanine-nucleotide exchange by Cdc24 and stimulation of GTPase activity by Bem3. J. Biol. Chem. *269*, 2369–2372.

Ziman, M., Obrien, J. M., Ouellette, L. A., Church, W. R., and Johnson, D. I. (1991). Mutational Analysis of Cdc42Sc, a *Saccharomyces cerevisiae* gene that encodes a putative GTP-binding protein Involved in the control of cell polarity. Mol. Cell. Biol. *11*, 3537–3544.